Earth-Science Reviews, Volume 95, Issues 3-4, August 2009, Pages 158-188

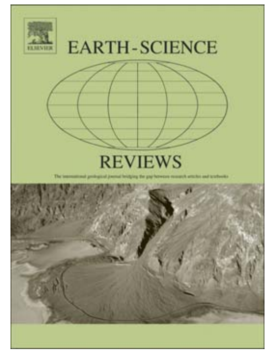

Accepted Manuscript

Controlling factors for the spatial variability of soil magnetic susceptibility across England and Wales

A. Blundell, J.A. Dearing, J.F. Boyle, J.A. Hannam

PII: S0012-8252(09)00081-6
DOI: doi: 10.1016/j.earscirev.2009.05.001
Reference: EARTH 1568

To appear in: *Earth Science Reviews*

Received date: 25 April 2008
Revised date: 21 April 2009
Accepted date: 13 May 2009

Please cite this article as: Blundell, A., Dearing, J.A., Boyle, J.F., Hannam, J.A., Controlling factors for the spatial variability of soil magnetic susceptibility across England and Wales, *Earth Science Reviews* (2009), doi: 10.1016/j.earscirev.2009.05.001

Controlling factors for the spatial variability of soil magnetic susceptibility across England and Wales.

Blundell, A.[a1], **Dearing, J.A.** [a2], **Boyle, J.F.** [a]

[a] Department of Geography, University of Liverpool, Liverpool L69 7ZT, United Kingdom

(a.blundell@leeds.ac.uk; j.dearing@soton.ac.uk; jfb@liv.ac.uk)

Hannam, J.A. [b]

[b] Natural Resources Department, National Soil Resources Institute, School of Applied Sciences, Cranfield University, Cranfield, MK43 0AL, United Kingdom

(j.a.hannam@cranfield.ac.uk)

Corresponding author **A. Blundell** tel: +44 (0)113 343 3381; fax: +44 (0) 113 343 3308

[1]Present address: School of Geography, University of Leeds, Leeds LS2 9JT, UK.

[2]Present address: School of Geography, University of Southampton, Southampton SO17 1BJ, UK.

Abstract

We review the nature and importance of soil factors implicated in the formation of secondary ferrimagnetic minerals in soils and palaeosols worldwide. The findings are examined with respect to temperate regions through a comprehensive analysis of over 5000 samples of surface soil from England and Wales taken from a 5 x 5 km grid. Over 30 soil and environmental attributes are considered for each sample as proxies for soil forming factors. Measurements of low field magnetic susceptibility (mass specific) and frequency-dependent susceptibility (mass specific and percentage) on each sample provide estimates of the concentration and grain size of ferrimagnetic minerals.

Maps of soil magnetism across England and Wales show non-random distributions and clusters. One sub-set of data is clearly linked to contamination from atmospheric pollution, and excluded from subsequent analyses. The concentration of ferrimagnetic minerals in the non-polluted set is broadly proportional to the concentration of minerals falling into the viscous superparamagnetic domain size range (~ 15 - 25 nm). This set shows clusters of high magnetic concentrations particularly over specific parent materials such as schists and slates, mudstones and limestones.

Bivariate analyses and linear multiple regression models show that the main controlling factors are parent material and drainage, the latter represented by soil drainage classes and particle-size. Together these two factors account for ~ 30 % of the magnetic variability in the complete dataset. A second group of factors, including climate (mean annual rainfall), relief (slope and altitude), and organisms (land use, organic carbon and pH) have subordinate control. Climate as represented by mean annual temperature and pedogenic time is deemed not relevant at these spatio-temporal scales.

The findings are consistent with a largely abiotic system where the role of iron-reducing bacteria appears minor. At coarse spatial and temporal scales, secondary ferrimagnetic mineral formation is controlled by the weathering capacity to supply Fe to the surface soil. At finer scales, soluble Fe precipitates as ferrihydrite before transformation in response to periodically anaerobic conditions into other minerals including nanoscale magnetite.

Keywords

Soil magnetism; Magnetic susceptibility; Frequency-dependence; Soil forming factors; England and Wales

1. Introduction and aims

Magnetic properties of soils are commonly used in earth and environmental sciences in diverse ways (Thompson et al., 1980; Thompson and Oldfield, 1986): as 'fingerprints' of sediment sources in fluvial, limnic and marine sediments (eg. Thompson et al., 1975; Walling et al., 1979; Dearing et al., 1985; Bloemendal et al., 1988; Dearing, 1999, 2000); as records of atmospheric pollution (Oldfield et al., 1978; Hay et al .,1997) as tools for archaeological mapping and prospecting (eg. Tite and Mullins 1970; Dalan and Banerjee 1996); as a climate proxy in loess-palaeosol sequences (eg. Heller and Liu 1986; Liu et al., 1995; Maher and Thompson, 1995); as proxies for planetary atmospheric conditions (Retallack et al., 2003; Barrón and Torrent, 2002); and as an aid to detecting land mines using electromagnetic techniques (Hannam and Dearing, 2008). Despite the widespread use and application the mechanisms of magnetic mineral formation in soils remain ambiguous.

The most debated concept is 'magnetic enhancement' whereby topsoils in temperate, Mediterranean, steppe, sub-tropical and tropical zones may show higher values of magnetic susceptibility than subsoils: a feature first observed in temperate soils more than 50 years ago (Le Borgne, 1955). Since then several theories have sought to explain the chemistry, physics and formation of the minerals that commonly produce the enhanced magnetic effect. Le Borgne (1955), and later Mullins (1977), suggested the dominant process was 'fermentation' whereby wetting and drying cycles within the soil profile would allow the bioreduction of Fe in anaerobic conditions, followed by the precipitation of magnetite (Fe_3O_4) or maghemite (γ-Fe_2O_3). Early attempts to simulate the process in the laboratory (Maher and Taylor, 1988) showed that fine-grained magnetite could be produced in the absence of Fe-reducers, suggesting that magnetic enhancement in soils involves the competitive abiotic interplay of mineral formation

(Maher, 1998). Le Borgne (1960) also observed magnetic enhancement by fire and deduced that thermal transformation of weakly magnetic Fe minerals to ferrimagnetic magnetite/maghemite took place as the soil atmosphere shifted from aerobic to anaerobic as the fire developed, and back to aerobic as the soil cooled. Subsequent field studies found evidence for the pedogenic production of bacterial magnetosomes (Fassbinder et al., 1990) and the ferrimagnetic iron sulphide, greigite (Stanjek et al., 1994) in certain poorly drained soils.

Dearing et al. (1996a) tested several theories of secondary ferrimagnetic mineral (SFM) formation in temperate soils by creating and analysing maps of low field magnetic susceptibility and frequency-dependent susceptibility of soils across England. This study was based on measurements of the UK National Soil Resource Institute's (NSRI) National Soil Inventory (NSI) sub-sampled at 10 km grid intersections. The maps showed that the majority of soils had magnetic properties dominated by the presence of nanoscale superparamagnetic (SP) and stable single domain (SSD) grains produced in situ, collectively termed SFMs. Primary ferrimagnetic minerals (PFM) derived from geological sources, the effects of fire, and accumulation of atmospheric pollution particles (Oldfield et al., 1978; Hay et al., 1997) from fossil-fuel burning were found to dominate surface magnetic properties in only a minority of localities.

From this analysis, a conceptual model of SFM formation in temperate regions was constructed that describes the interactions between different environmental factors and biogeochemical processes responsible for the magnetic patterns observable at different spatial and temporal scales (Figure 1). As with other soil properties, controls on soil magnetic variations may be viewed in terms of environmental factors or boundary conditions that constrain the dynamic processes of mineral formation and accumulation. The model suggested that at the spatio-temporal scale represented by regional landscapes and glacial-interglacial cycles, the first order factors are climate and soil parent material. Following the work and theories of Schwertmann (1988) and Schwertmann and Taylor (1989), these conditions combine to control the flux of soluble Fe (FeII) and the production of reactive hydrous ferric oxides, such as ferrihydrite (5Fe-$_2O_3$. $9H_2O$) in the soil. A second phase, the transformation of ferrihydrite into more crystalline minerals, may involve Dissimilatory Iron Reducing Bacteria (DIRB) in the reduction of FeIII to FeII with the interaction of excess FeII and ferrihydrite producing SP and SSD magnetite. Maghemite may also be formed through relatively short-term oxidation and transformation from magnetite. At local spatial scales, vegetation, land use and relief set conditions for soil chemistry, structure and drainage. These may operate positively on the formation and accumulation of SFMs, for example through allowing fluctuating redox cycles, or impose constraints through the effects of destructive chelating and gleying processes (see Supplementary Information for definitions of soil terms).

These proposed factors and processes are largely in line with the earliest theories that relate to fermentation processes (Le Borgne, 1955; Mullins, 1977), and are also supported by subsequent empirical studies that quantify the secondary ferrimagnetic grain-size using low temperature magnetic measurements (eg. Dearing et al., 1997) and constrain the contributions of bacterial magnetosomes in highly magnetic soils on the basis of soil DNA analysis (Dearing et al., 2001a). Other workers have followed the laboratory findings of Maher and Taylor (1988) and provided strong evidence from field and laboratory studies to counter a dominant biomineralization scheme, especially in Mediterranean soils. These studies support a theory of abiotic ageing of ferrihydrite to hematite through the intermediate mineral hydromaghemite as a major pathway of magnetic enhancement (Barrón et al., 2003; Torrent et al., 2006; Liu et al., 2008). Extrapolation of laboratory studies (Barrón and Torrent, 2002) suggests that complete transformation of maghemite to hematite at room temperature takes place within 1 Ma.

This paper describes the first phase of analysis in a project designed to generate predictive modelling tools for SFMs in temperate soils. It reviews the role of broad soil forming factors in constraining the spatial patterns of magnetic susceptibility and frequency-dependent susceptibility in soils across England and Wales, evaluating the significance of factors in both univariate and multivariate terms. Other national/sub national scale soil magnetic datasets exist in the Czech republic and/or Austria (Fialova et al., 2006; Hanesch et al., 2001; 2007), Germany, Czech republic and Poland (Magiera et al., 2006), Estonia (Bityukova et al., 1999) but these have been used primarily to examine the applicability of magnetic measures for detecting signs of pollution (Bityukova et al., 1999; Boyko et al., 2004; Magiera et al., 2006; Hanesch et al., 2007). Several of the studies have addressed the contribution of geology and, in the case of Hanesch et al. (2001), the effect of different land uses is also reported via the use of fuzzy c-means cluster analysis. However, the multivariate nature of relationships between soil forming factors and soil magnetic properties have not been systematically analysed within these studies. Here, we utilize the same NSRI soil inventory set for England used by Dearing et al. (1996a) but at a higher resolution of 5 km grid samples extended to cover both England and Wales, and with a considerably extended set of soil attributes allowing a more comprehensive analysis of the role of soil forming factors.

An inductive approach with no *a priori* assumptions about causality is adopted to explore the relationships between soil forming factors and the production or destruction of SFMs in topsoils in England and Wales, primarily at a spatial scale set by the 5 km grid sampling interval over a whole area equivalent to ~150 000 km^2. Datasets of magnetic measurements and environmental attributes related to each geo-referenced sample point are analysed through ranking, bivariate plots, comparative analyses of sub-sets, and where possible through multiple regression statistics.

2. Soil forming factors and magnetism

Factors of soil formation as outlined by Jenny (1941) are used conventionally to provide a framework within which to analyse the variability of soil properties.

$$S = f(Cl,O,R,P,T)$$

S= Soil, Cl= Climate, O = Organisms/Vegetation, R = Relief, P= Parent material, T=Time

In theory, the Jenny equation can be used to explain the role of individual environmental factors on a soil attribute but in practice the factors are normally inter-dependent. The following paragraphs review current knowledge about the role of each factor on soil magnetism.

2.1 Parent material

There are at least four aspects in which parent material operates as a factor for soil magnetism. First, a supply of Fe from parent material is essential for SFM production which is, at least partly, dependent upon the rate of weathering driven by hydrolysis, oxidation and reductive dissolution. In England, the Fe-rich Jurassic limestones, Cretaceous Lower Greensands and Devonian slates and were reported by Tite (1972) as being the geologies likely to produce the most magnetic enhancement. But parent materials with low Fe concentrations that are able to weather at a high rate, such as chalk, may in theory effectively produce sufficient Fe for substantial ferrimagnetic enhancement (cf. Mourkarika, Obrien and Coey, 1991). Second, high concentrations of ferrimagnetic minerals in surface soils may result through the accumulation of resistant PFMs through weathering of igneous rocks (eg. Singer and Fine, 1989), and even in sedimentary rocks (eg. chalk) where magnetic grains exists as inclusions in biogenic quartz (Vali et al., 1989; Hounslow and Maher, 1996). Third, resistant metamorphic and sedimentary rocks, as in the UK, are often co-correlated with elevated topography and as a result are also associated with lower temperatures and elevated orographic rainfall. Fourth, parent material influences many of the physical and chemical soil conditions, such as texture, drainage and pH.

2.2 Climate

Many studies have attempted to identify the climate controls on soil and palaeosol magnetism, spurred by the potential opportunity to reconstruct palaeoclimate in loess sequences. The effects of rainfall have been widely reported as an important causal factor in the magnetic enhancement of paleosols, for example, in the Loess Plateau in China (Maher and Thompson, 1995), the Russian steppe (Maher et al., 2002) and the Matmata Plateau, Tunisia (Dearing et al., 2001b). Crucially, these are areas where other soil forming factors are held relatively constant apart from time (Vidic et al., 2004). Palaeosol susceptibility records from the N. Hemisphere by Maher and Thompson (1995) demonstrated a trend of increasing susceptibility with annual rainfall from 200 mm to a peak around 1500 mm, followed by a decline to ~3000 mm. A similar peak (~1000 mm) in susceptibility was observed in soils from Hawaii (Singer et al., 1996). Increased humidity, resulting from greater rainfall and lower evapotranspiration, in Saskatchewan was suggested by de Jong et al. (1999) to be important in determining the highest magnetic susceptibility values found in Gray Luvisols and Dark Gray Chernozems. These observations are consistent with Dearing et al.'s (1996a, 2001b) argument that the major role of rainfall lies in terms of driving hydrolysis reactions and the release of Fe from primary minerals.

A study of modern soil magnetic variability across four regions of China (Loess plateau, South China, Qinghai-Xizang and North-west China) was able to demonstrate interactions between mean annual temperature (range -4 to 24°C) and mean annual rainfall (range 10-2000 mm) in controlling modern soil magnetism (Han et al., 1996). But generally, the effects of temperature are less well studied and would seem less pronounced, although laboratory studies by Barrón et al. (2003) suggest that temperature may be a key factor in magnetic enhancement driven by ferrihydrite conversion to maghemite. In England and Wales, there are marked gradients of rainfall from west to east, largely related to both the prevailing westerly airstreams and greater altitude in the west. Temperature variations are also related to altitude, together with latitude and the proximity to the coast. However relatively narrow ranges of mean daily temperature between 4.2 – 11.5 ^{0}C and mean annual precipitation 517 – 4134 mm (with 70 % of sites < 950 mm) suggest the influence of climate should be more limited.

2.3 Relief and drainage

Relief is important with respect to magnetic enhancement because it is intimately linked with soil drainage and translocation of soil particles. Magnetic studies of catena sequences show different relationships depending on the dominant particle size of the main magnetic fraction. Commonly susceptibility increases down slope on a variety of parent materials related to increasing soil fines (eg. Thompson and Oldfield, 1986; de

Jong et al., 1998), but was shown to decrease when coatings on coarser sand-sized particles were the main carriers of the pedogenic magnetic material (de Jong et al., 2000). Peak susceptibilities were also observed on slope crests in the English Chiltern Hills with low values on more eroded steep slopes (Dearing, 2000) suggesting that the rates of erosion exceeded rates of magnetic enhancement.

The degree of drainage controls soil redox conditions, which in turn is expected to affect bacterial activity, as well as abiotic chemical reactions affecting Fe-minerals. Ferrimagnetic minerals in soils experiencing prolonged waterlogging (gleying) appear to undergo reductive dissolution under anaerobic conditions (Mullins, 1977; Thompson and Oldfield, 1986; Maher, 1986; Dearing et al., 1995; de Jong et al., 2000) resulting in substantial decreases in magnetic concentrations in gleyed horizons. In contrast, highly porous soils appear to constrain SFM production because either the levels of micropores are too low to permit fermentation processes or that Fe-minerals are removed from the profile either as a result of excessive Fe leaching or chelation under acidic conditions (Maher, 1986; Dearing et al., 1985, 1995, 1996a).

2.4 Soil organisms and vegetation

Within the soil profile, organisms may have a variety of effects on magnetic mineral formation. The efficiency of a fermentation mechanism is expected to depend on the population and activity of DIRB. These heterotrophic bacteria require moderate temperature (>10 °C required for significant activity), adequate moisture, organic carbon (acetate and other short-chain fatty acids) as electron donors, and intermediate to alkaline pH. These are conditions that are often best met within the rhizosphere, rather than the bulk soil. Low levels of organic matter might therefore represent limiting conditions, as perhaps illustrated by Neumeister and Peschel's (1968) data from

Germany that show a positive relationship between soil magnetic susceptibility and organic levels in arable soils. Therefore, land use and vegetation may play significant roles in determining the nature of microorganism-mineral interaction through controls on the nature and size of the rhizosphere. Additionally, land use and vegetation are expected to exert a control on chelation and acid weathering, and hence the activities of certain processes, such as podzolisation, that may be detrimental to magnetic mineral formation and accumulation. Macroorganisms, such as earthworms and moles, have potentially a large role in controlling the distribution of minerals through continuous bioturbation, especially the physical coupling of surface soil and the weathering zone. Land use as a major control on vegetation and soil disturbance, especially in a heavily managed region like England and Wales, may also be expected to control locally the distribution and intensity of fire, soil drainage, soil mixing through ploughing and soil chemistry though application of manures and conditioners. With regards the possible effects of fire, Dearing et al. (1996a) found highest mean susceptibility values in ley grassland and arable soils, but were unable to make any link between these spatial distributions and crop burning despite a long history of this land management practice. Substantial conversion from non-ferrimagnetic to fine grained ferrimagnetic material may occur above 400 °C but most significantly above 550 °C (Rummery et al., 1979). However, these temperatures are not always reached (Rasmussen et al., 1986) and insufficient organic matter and soil Fe may mean that the spatial effect is uneven (Maher, 1986). The historical contribution of pyrogenic ferrimagnetic particles within the topsoil may also be complicated by bioturbation, ploughing, dissolution, and post-fire erosion (Blake et al., 2005) making evidence of fire difficult to separate from that of natural topsoil magnetic enhancement. Oldfield and Crowther (2007) report that magnetic enhancement forced predominantly by fire can be detected using additional measurements of anhysteretic magnetic susceptibility.

2.5 Time

Like all pedogenic processes, magnetic enhancement is time dependent but few studies provide conclusive data for rates of mineral formation. Magnetic measurement of soil chronosequences on river and marine terraces in the Mediterranean (Torrent et al., 1980) and California (Singer et al., 1992) have shown increasing enhancement with age. Singer et al. (1992) reported that susceptibility had shown continued enhancement for over 240,000 years. These changes were attributed to the greater cumulative effects of the weathering of parent material and release of Fe bearing minerals for potential conversion to SFMs. However, in China, susceptibility values of similar magnitude exist for modern loess soils and palaeosols, the latter often having experienced substantially longer duration of pedogenesis (Maher and Thompson, 1995). While this suggests that magnetic susceptibility may attain 'saturation' status rapidly within a few hundred to a few thousand years (Maher and Thompson, 1995), other views emphasize the interactions between climate and time (eg. Vidic et al., 2004). Where SFMs form via a pathway that ultimately ends in non-ferrimagnetic minerals, like hematite (eg. Barrón and Torrent, 2002), there clearly must be an optimum period for the production of ferrimagnetic minerals under a given set of environmental factors.

Laboratory experiments run under strictly anaerobic conditions have demonstrated the production of ferrimagnetic minerals over short timescales (days to months) using both Fe enriched soil (Hanesch and Petersen, 1999) and bacterial growth media (eg. Hansel et al., 2003). However, the extent to which these studies are analogues for real soil environments is not clear. Attempts to simulate the rate of magnetic enhancement in microcosms representing ambient soil environments have not been straightforward (Hannam, 1999; Dearing et al., 2001a). In contrast, it is fairly easy to show the rapid rate

(10^0-10^1 years) of destructive processes in the laboratory and field caused by permanent waterlogging (Hannam, 1999; Dearing et al., 2001a). England and Wales have been affected by glaciations during which pedogenesis has often been interrupted or completely halted, yet some of the southern regions escaped ice coverage. Therefore, there are opportunities in the present study to assume that pedogenic processes and magnetic enhancement were able to start from effectively 'time zero' in different areas over different time periods.

3. Methods and Techniques

3.1 Field sampling and sample analysis (see also Supplementary Information)

Soil samples from the NSI archive have been employed in this project. Field sampling of soils for the NSI was originally undertaken at sites 1000 m north and 1000 m east of 5 × 5 km grid intersections (based on the UK Ordnance Survey National Grid) across England and Wales by soil surveyors between 1978 and 1982, with some later re-sampling in the mid 1990s. At each site, a total of 25 soil cores to a depth of 15 cm from within a 20 × 20 m grid were amalgamated together in the field, and a single soil pit was dug and described using standard procedures (Hodgson, 1976). All litter, fermentation and humus layers were excluded from the samples. Samples were air dried, ground to pass through a 2 mm sieve and subsequently archived in plastic bags at room temperature. Laboratory analyses were undertaken for soil particle size, pH, organic carbon and 18 chemical elements derived by aqua regia digests (4:1 hydrochloric:nitric acids by volume), however for this publication only Fe was employed. pH was measured with a pH meter in a 1:2.5 dilution with de-ionized water (McGrath and Loveland, 1992).

Soil particle size analysis on the <2mm fraction was achieved using the pipette method (Avery & Bascomb, 1974)

A previous magnetic dataset (containing susceptibility and frequency dependence measures) of 1955 samples (Dearing et al., 1996a) has been supplemented by measurements on 3701 further samples to produce a complete magnetic susceptibility dataset at a 5 × 5 km resolution across England and Wales. In both studies, volume based magnetic susceptibility was measured at both low and high frequencies (470 Hz and 4700 Hz) on 10 ml samples using a Bartington Instruments dual frequency MS2B sensor, and expressed as mass specific magnetic susceptibility (χ_{LF} 10^{-6} m^3 kg^{-1}), mass specific frequency dependent susceptibility (χ_{FD} 10^{-9} m^3 kg^{-1}) and percentage frequency dependent susceptibility (χ_{FD}%). Typical ranges for broad geologies, sediments and soils are quoted in Thompson and Oldfield (1986) and also Walden et al. (1999). Thirty one archived samples had insufficient material to analyse. Following data entry, values were extensively checked for outliers reflecting possible operator error and, where necessary, samples were re-analysed. Samples from the earlier studies were also re-analysed to ensure that no significant changes in magnetic measures were evident due to the effects of prolonged storage. Comparison of previous and new measurements for 70 samples revealed r^2 values for χ_{LF} and χ_{FD} of 0.99 and a slope of 1.0004 for both, thus confirming no significant time-related changes.

Thirty repeated measurements of both volume susceptibility ($\kappa_{LF} \times 10^{-5}$) and χ_{FD} % values for 10 samples that represent the range of values across the dataset serve to illustrate (Figure 2) the relationship between the magnitude of κ_{LF} and the uncertainty of calculated χ_{FD}% values. The 95% confidence interval widens disproportionately as κ_{LF}

reduces in magnitude. At κ_{LF} = 10, χ_{FD} % values have a precision of ± 2 % units (equivalent to a relative uncertainty of ±15% assuming maximum χ_{FD} % = 14). This degree of precision is similar to that set by Dearing et al. (1996a). We therefore use a threshold value of κ_{LF} = 10 to exclude samples with unacceptably low levels of precision (n = 377; 7 % of original dataset; n = 5656). Samples with very high χ_{FD} % values (~ 14%) were reanalysed and confirmed.

Soils receiving atmospheric pollution may be magnetically contaminated by a range of Fe-rich particles derived from metalliferous industries (Ďurža, 1999) and fossil fuel combustion (Flanders, 1994; Kapička et al.,1999; Magiera and Strzyszcz, 2000). Following the approach taken by Hay et al. (1997), we use the combined thresholds of χ_{FD} % <3% and the median of the dataset (χ_{LF} > 0.38) to identify a potentially heavily polluted sub-set (n = 637, 11% of original magnetic dataset).

3.2 Datasets of soil factors

Soil parent material was obtained from Information of both bedrock and superficial cover sourced from DiGmAPgb-50 under licence from the British Geological Survey (BGS Digital Licence 2006/134ed). At 1:50 000 not all data are available for Wales and therefore lower resolution data were used to assign data to our soil locations from either 1:250 000 (bedrock geology) or 1:625 000 for superficial geology where necessary. A total of 151 rock types and 174 superficial cover types are distinguished, but for the purposes of this study these have been aggregated into 44 and 22 broad compositional types of *Parent Material*[1] respectively (Figure 6a-b). If the bedrock has a superficial covering, for example till, it is the superficial cover that is recorded here as *Parent*

[1] Names of data attributes/variables are shown in italics.

material. Climate is derived from spatially interpolated long term (1961-1990) average climate datasets, adjusted for altitude, from the UK Meteorological Office (Perry and Hollis, 2004; http://www.metoffice.gov.uk/) provide values of mean annual rainfall (*MAR*, mm) and mean annual temperature (*MAT*, °C), reduced to 12 classes each for box plots.

Locations covered in the NSI soil collection possess a series of attribute data including standard recordings detailed in the Soil Survey Field Handbook (Hodgson, 1976; www.landis.org.uk/gateway/ooi/nsi.cfm) including assessment of soil type. Relief represented by slope angle degrees (*Slope*) and altitude (*Alt*) above sea level (m asl). The soil attribute *Texture,* providing proxy data for porosity and drainage, is reduced from 53 categories to 13 as many of the original categories had less than 5 occurrences. Specific diagnostic features indicative of waterlogging within the soil profile include the presence of mottles and gleying. All soil types are classified into four broad classes of depth to mottling (*Drainage index*) representing poorly drained, poor-intermediate, intermediate-free and freely draining. Vegetation/soil organisms are assessed by the proxies *Land Use*, organic matter (*%OC*) and pH.

The factor of *Time* is addressed by comparing data within zones delimited by glaciation. Area 1 south of the Anglian limit, area 2 between the Anglian and Devensian limits and area 3 north of the Devensian limit are assumed to provide minimum durations of pedogenesis of > 480 000 years, 350 000 years and ~ 10 000 years respectively.

3.3 Data analysis

Missing data and excluded samples result in different numbers of samples across three databases. We refer to a 'complete' dataset, with entries in all the soil and environmental variables (n = 5538), a 'polluted' dataset (n = 637) defined by two threshold magnetic measurements, and a 'reduced' dataset that excludes the polluted samples, samples with incomplete soil attribute data entries and five other samples with unexplained negative χ_{LF} values. The 'reduced' subset comprises 4896 samples for χ_{LF} measurements and 4535 samples for χ_{FD} and χ_{FD} % measurements and is used for the majority of analyses below.

Statistical transformations of continuous data are used to derive distributions as close to normal as possible. Thus $\log_{(10)}$ transformed variables include χ_{LF} (*log*χ_{LF}), χ_{FD} +1 (*log*χ_{FD}) (Figure 3) *logMAR*) slope angle +1 (*logSlope*), %OC + 1 (*logOC*) and Altitude + 2 (*logAlt*). Mean annual temperature *MAT* data were reflected and then log $_{(b10)}$ transformed (*logrMAT*). Variables with constant units added to all their values have negative or 0 minimum values meaning that 'started log' transformations are required (Cohen et al., 2003). Particle size data (carried out on samples with OC% < 15) have also been transformed as necessary with either $\log_{(10)}$ or square root functions.

The SPSS statistical package is used to determine the directions and strengths of relationships between soil factors and magnetic parameters. Soil factor variables exist as either continuous (eg. *MAR*) or category (eg. *Parent material*) datasets. For some analyses, continuous data are placed into classes to enable the production of box plots. The analyses comprise: A) Soil factor variables are ranked according to mean magnetic values for each attribute category (text) or percentile class (continuous data). B) Some data distributions are displayed using box plots and tables derived from classifying numeric continuous data based on percentiles where class 1 is 0 – < 10 percentile, class 2 is ≥ 10 percentile - < 20 percentile etc. up to class 9, but where classes 10, 11 and 12 equate to boundaries dictated by the 90, 95, 98 and 100 percentile values. This is not the case for slope angle where, based upon the histogram observed and heavy skew towards low slopes, 6 classes were derived. C) Relationships between continuous data (eg. *MAR*) and magnetic parameters are examined using standard scatter plots with superimposed 250 sample running means to show underlying trends together with box plots (see Supplementary Information). D) For some nominal/ordinal based factors, scatter plots of category mean magnetic data versus individual sample magnetic data are employed to show and calculate the strength (Pearson moment correlation coefficient) of statistical association. E) Some analysis of variance (ANOVA), including *post hoc* tests, and t-tests are employed to determine whether differences between class/category means are significant. F) In order to determine the degree of linear correlation, correlation coefficients are also calculated. G) Standard multiple regression models are applied to three datasets that vary in sample selection. The nonlinear nature of magnetic associations with organic carbon means it was necessary to derive three models with different data configurations.

In order to test for correlations between the magnetic parameters and the environmental factors, it is necessary to express the environmental variables in an appropriate quantitative form. For continuous data such as *MAR* and *MAT* it has simply been a matter of transformation to avoid skew. However, for the category data this is not possible, and we have chosen instead to assign indices to each category calculated from the observed magnetic parameter values as shown visibly, for example, for *Parent material* (Figure 7). Thus for χ_{LF}, the index for the parent material Chalk is simply the mean χ_{LF} value of all samples located on chalk. The relative importance of *Parent material* as a predictor of χ_{LF} can then be tested by the relative magnitude of the correlation coefficient. Because magnetic parameters are being compared with both categorical and measured quantitative data, it is important to rule out the possibility that categorisation biases the results. All of the data were categorised and there was no substantial change in the order of importance of factors with regards to partial correlations (see Supplementary Information).

4. Magnetic patterns and soil factors

4.1 Magnetic data

The complete dataset of χ_{LF} (× 10^{-6} m^3 kg^{-1}) values (n = 5656) spans three orders of magnitude (-0.01 - 32.70) but is highly skewed towards the median of 0.37 with only 2 % of values greater than 6.29 (Table 1). Values of χ_{FD} (× 10^{-9} m^3 kg^{-1}) also cover at least three orders of magnitude (0.00 - 2329.32) and are positively skewed. Values of χ_{FD} % exhibit a more normal distribution with values between 0 and 13.6 % and are therefore not transformed. The reduced dataset (Table 1) has a lower median χ_{LF} value of 0.32 but elevated median values for both χ_{FD} and χ_{FD} % of 14.37 and 4.07 respectively. Typical ranges of χ_{LF}, χ_{FD} and χ_{FD} % measurements for broad geologies and sediments are quoted in Thompson and Oldfield (1986) and Walden et al. (1999), but notably the ranges of data for surface soils from England and Wales span a significant range of the published global range, including soils from Mediterranean and tropical areas (Dearing et al., 1996b; Dearing and Hannam, submitted).

Only 5 % of the samples show χ_{LF} < 0.1, indicating that the magnetic susceptibility of 95 % of soils is dominated by the presence of ferrimagnetic minerals, such as magnetite and maghemite, rather than paramagnetic and canted anti-ferromagnetic minerals (eg.

ferrihydrite, goethite and hematite). Of the ferrimagnetic soils, 74.8 %, 44.7 %, 26.3 %, 12.7 % and 3.73 % have χ_{FD} % values greater than 2, 4, 6, 8, and 10 respectively demonstrating that viscous superparamagnetic (VSPM) grains of magnetite/maghemite are present in > 75 % of samples and make significant contributions to the magnetic volume in > 50 % of the whole sample set (cf. Mullins, 1977; Maher, 1986; Dearing et al., 1996a; Dearing et al., 1997; Dearing et al., 2001a).

Bivariate plots (Figure 3a-f) of the three parameters (normal and log transformed) show positive associations. The plots of logχ_{LF} and χ_{LF} versus χ_{FD} % (Figure 3a and b) exhibit a dominant cluster of points where χ_{LF} < 2 across the whole range of χ_{FD} % values. Two smaller clusters of points where χ_{LF} > 2 exist for ranges of χ_{FD} % values > 9 and < 3. The latter cluster corresponds to polluted samples excluded from further analysis. Correlations show r^2 values of 0.56 (logχ_{LF}) and 0.29 (χ_{LF}) for the non-polluted datasets. The shape of these plots suggests a 'saturation' distribution of ferrimagnetic minerals (SP-VSPM-SSD) equivalent to maximum χ_{FD} % values ~12 %. The plots of logχ_{FD} and χ_{FD} versus χ_{FD} % (Figures 3c and d) show r^2 values of 0.82 and 0.31 respectively, indicating that the distribution of ferrimagnetic grains (χ_{FD} %) is more strongly related to the concentration of VSPM grains (χ_{FD}) than the total concentration of all ferrimagnetic grains (χ_{LF}). The strongest correlations exist for logχ_{LF} and χ_{LF} versus χ_{FD} (Figures 3e and f) at 0.89 and 0.96 respectively. The strength of these relationships confirms that the total concentrations of ferrimagnetic minerals (χ_{LF}) is very closely related to the concentration of VSPM grains (χ_{FD}).

4.2 Magnetic spatial patterns

Comparison of maps of place names / geographical features (Figure 4a) and magnetic patterns of χ_{LF}, χ_{FD} and χ_{FD}% (Figure 4b-d) shows a number of regional clusters of high magnetic values (> 1.0). These features are broadly repeated for each parameter. The largest clusters cover much of southwest England (counties of Devon and Cornwall) where the mean value (χ_{LF} = 3.04) is more than three times the dataset average. The relatively high values of χ_{FD}% in Devon and Cornwall ($\bar{x}$ = 7.56) suggest that many are dominated by VSPMs (cf. Dearing et al., 1997). There are smaller clusters of high χ_{LF} values in lowland England on the Cotswolds Hills, Salisbury Plain, the counties of Wiltshire, Dorset, and Cambridgeshire, and to a lesser extent the North and South Downs, and Lincolnshire and Yorkshire Wolds. The distribution of χ_{FD} values is similar to χ_{LF} but highlights with even more clarity the association with uplands especially in SE England. Here the calcareous Chiltern Hills (NW of London), the Berkshire Downs (W of London) and North Downs (SE of London) are clearly identified by clusters of moderate χ_{FD} values. In Wales, high susceptibility areas in the south west (especially the county of Pembrokeshire) also have high levels of χ_{FD} and χ_{FD}%.

In contrast, the sandstone Wealden hills to the south of London and the crystalline hills of the Malvern Hills are magnetically indistinct. Clusters of low χ_{LF} values (< 0.10) are also found on the granitic Dartmoor massif in SW England, the New Forest in Hampshire, SE Dorset, central and southern Wales, the Pennine upland chain north of Skipton extending to the Scottish border, the Cheviot Hills, and in northern, central and south Wales. All these areas are typified by organic rich soils at relatively high altitudes or low-lying poorly drained areas. However, the lowland peat areas of the Somerset Levels, and the Fens of Cambridgeshire and Lincolnshire do not fall into this cluster with many samples showing moderate values of χ_{LF}.

Smaller clusters of elevated χ_{LF} values are also related to major industrial areas where the conspicuous lack of high χ_{FD} % values suggests potential domination by atmospheric pollution particles. The spatial distribution of the threshold defined polluted dataset (Figure 5) exhibits clusters of polluted topsoils around the urban areas of Newcastle, Middlesbrough, Hull, Leeds, Merseyside, Manchester, Northern Birmingham, London, Nottingham and Derby. In Wales, the polluted dataset maps on to the mining valleys of South Wales. Other samples from the polluted dataset are found in more rural regions in Devon and Cornwall, Mid and North Wales, Lincolnshire, Yorkshire, Cumbria and Northumberland. Sites on igneous or ultramafic parent materials dominated by PFMs may have similar magnetic thresholds that are used to define the polluted data set. However, 94 % of sites on igneous bedrock, from the complete dataset, do not meet the threshold criteria for pollution. Only 10 samples in the 'polluted sub-set' (1.5 % of all 'polluted' subset) overly igneous rock. This strongly underlines the association between the total concentration of highly magnetic minerals and the presence of VSPM, rather than PFM grains.

4.3 Association with soil factors

Further analyses and figures (S1-S12) of the associations between magnetic parameters and individual soil attributes for the main soil factors are provided in the Supplementary Information. Here we examine the main most important findings.

Parent Material

After ranking, *Schist or slate*, *Limestone-ooidal* (Jurassic) and *Mudstone-Palaeozoic (P)* occupy the top three places for all magnetic measurements with *Mudstone and* *sandstone (P)*, *Sandstone and mudstone (P)* and *Sandstone (P)* consistently in the top ten places (Table 2). These parent materials cover much of Devon and Cornwall in SW England, SW and Mid-west Wales and are also common around the mining areas of Nottinghamshire in central England (Figure 4a; Figure 6a-b). The lower rankings consist of many superficial parent materials such as *Till-preDevensian*, *Alluvium*, *Tidal flat*, and variations of *Clay/silt/sand* and *Peat*. On average samples exhibit higher $\log\chi_{LF}$ values where there is no superficial cover ($\bar{x}$ = -0.286, se = 0.011) than where there is superficial cover ($\bar{x}$ = -0.490, se = 0.007), and this difference is significant (t(3949.5df) = -15.498, $p < 0.05$) but not especially strong (r = 0.24). Similarly, values of χ_{FD} % are higher where there is no superficial cover ($\bar{x}$ = 5.42, se = 0.07) than where there is superficial cover ($\bar{x}$ = 3.9, se = 0.05), also showing a significant difference (t(3839df) = 18.37, $p < 0.05$, r = 0.28).

The strong association between magnetic values for each soil sample and the mean for each *Parent material* is demonstrated in Figure 7 a – c with r values of 0.48, 0.51, and 0.50 ($p < 0.05$) for $\log\chi_{LF}$, $\log\chi_{FD}$ and χ_{FD} % respectively.

Climate

MAR values (Table 3a) range from 517 – 4134 mm with 70 % of sites < 950 mm. There are no statistically significant bivariate linear relationships between *logMAR* and $\log\chi_{LF}$, $\log\chi_{FD}$ or χ_{FD} % (typically r = 0.05, $p < 0.05$). Values rise above 947 mm reaching peak means in the ranges *MAR* = 1109-1382 mm ($\log\chi_{LF}$ and $\log\chi_{FD}$) and *MAR* = 1382-1634 mm (χ_{FD} %). *MAT* values range from 4.2 °C to 11.5 °C (Table 3b), with 40 % of sites lying in the range 8.5 - 9.8 °C. There is a rise in mean magnetic values from 4.2 - 7.6 °C up to a peak values in the percentile 8.3 - 8.8 °C.

Relief and Drainage

Altitude ranges from 1 m below sea level to 1400 m above sea level with the majority (58 %) of sample sites lying between 50 m and 250 m. Mean values steadily rise from sea level to reach peak values in the ranges (Table 4a) 152 m to 206 m (logχ_{LF}) and 206 m to 310 m (logχ_{FD} and χ_{FD} %), but statistical correlations are either not significant or only weakly significant (r = not significant, r = 0.14, r = 0.16 respectively). Slope varies from 0° to 46° (Table 4b) with the distribution heavily skewed towards low values. Correlation coefficients between logχ_{LF}, logχ_{FD} and χ_{FD} % and *logSlope* are r = 0.14, 0.23 and 0.26 respectively with *logSlope* explaining most percentage variance (7 %) in χ_{FD} %. Soils developed upon flat or shallow slopes are associated with on average lower magnetic values, with peak values observed in the ranges 10° to 15° (logχ_{LF}), 15° to 20° (logχ_{FD}) and > 20° (χ_{FD} %).

Figure 8 and table 4c demonstrate that the highest mean magnetic values occur in free draining soils. Correlation coefficients between the mean magnetic value for each drainage class and the actual magnetic values reveal positive relationships of r = 0.38, 0.40 and 0.43 ($p < 0.05$) for logχ_{LF}, logχ_{FD} and χ_{FD} % respectively. Results of ANOVA (Welch test) show that there is a significant effect of *Drainage* on logχ_{LF}. (F(3, 1628.5df) = 274.8, $p < 0.05$, r = 0.38) and χ_{FD} % (F(3, 1519.47df) = 368.7 $p < 0.05$, r = 0.43) with Games Howell *post hoc* tests revealing that all drainage categories have means that are significantly ($p < 0.05$) different from each other for each magnetic parameter.

Sample counts for each *Texture* category are highly variable and despite 13 classes, *medium loams* and *medium silts* alone constitute 51 % of all samples. Ranking *Texture* categories (Table 5a) by mean logχ_{LF} values identifies the top four as *humose clays*, *medium loams*, *medium silts* and *light silts*. Frequency dependent parameters also show *medium loams* and *medium silts* ranked highly. The two lowest ranked categories for all the three magnetic parameters are *peats* and *humose sands.* Bivariate plots with particle-size data (measured where organic carbon < 15 %, n = 4206 for logχ_{LF} and n = 4104 for logχ_{FD} and χ_{FD} %) show similar patterns for most fractions (Figure 9). Values of logχ_{LF} fall either side of a peak at ~26 % for clay, 42 % for silt and 8 % for medium sand (*MSand*). Very fine sand (*VF Sand*) and medium fine sand (*MFSand*) display peak logχ_{LF} values at ~ 2 and 4 % respectively followed by a steady decline in logχ_{LF}. The exception is for log transformed coarse sand (*logCSand*) that shows significant ($p < 0.05$) linear and positive correlations with logχ_{LF} (r = 0.43), log χ_{FD} (r = 0.47) and χ_{FD} % (r = 0.43).

Organisms and vegetation

Land use categories are characterised by highly variable counts ranging from 4 (salt marsh) to 1631 (arable). Just two categories, *permanent grassland* and *arable*, represent 61 % of data set. *Ley grassland* is consistently the highest ranked land use type for all three magnetic parameters (Table 5b). The categories *scrub* and *arable* are ranked in the top six for all magnetic parameters. *Bog* and *upland heath* represent the largest categories in the bottom four places for each magnetic parameter. Values of *%OC* range from 0.1 to 65.5 (Table 6a), and 76 % of samples with logχ_{LF} values > 0 occur within classes 3 – 8 (*%OC* = 2.00 - 6.69). The 12 categories of *%OC* represent two major populations of soil: 1) peats (*%OC* > 12, classes categories 10 -12); and 2) non-peat soils (%OC ≤ 12 %; categories 1 - 9). T tests for unequal variances show that on average soils with *%OC* ≤ 12 have greater logχ_{LF} ($\bar{x}$ = -0.73, *se* = 0.02) than those with *%OC* > 12 % ($\bar{x}$ = -0.36, se = 0.01). The three magnetic parameters all show gradually rising values in running means with increasing values of *logOC*, up to ~0.6 - 0.8 (*%OC* = 3.5 - 4.2). All the magnetic parameters show low values in extremely acid

(pH < 4.0) and strongly alkaline (pH > 8.5) soils (Table 9b). The highest magnetic values exist in either moderately to slightly acidic soils (pH 4.0 - 6.0) or slightly alkaline soils (pH 7 – 8).

Time

General descriptive statistics for sample magnetic values in Area 1 (> 480 000 years), Area 2 (350 000 years) and Area 3 (~ 10 000 years) are displayed in Table 7. ANOVA analyses (Welch *F* ratio) show significant differences between means in logχ_{LF} data F (2, 3177.8df) = 42.43, $p < 0.05$, r = 0.141), log χ_{FD} data F (2, 2955df) = 41.9, $p < 0.05$, r = 0.136), and χ_{FD} % data F (2, 2943.4df) = 81.40, $p < 0.05$, r = 0.185). Games-Howell *post-hoc* tests reveal that all three areas have significantly different means. However, a generalised pattern of magnetic association with potential pedogenic time is difficult to discern. Mean values of logχ_{LF} are higher with increasing pedogenic time (Area 3 to Area 1), but this pattern is not repeated for logχ_{FD} and χ_{FD} % where mean values in Area 1 and Area 3 are higher than in Area 2. Area 1 has the highest proportion of its soils (24.4 %) with χ_{FD} % > 8, but Area 2 has only 4.7 % and Area 3 has 14.6 %.

5. Interacting soil factors

5.1 Correlation and multiple regression models

Considerations

The presence of large numbers of organic-rich soils presents an especially non-linear response with respect to the magnetic data. Thus statistical analyses for the whole data set (Model 1) are supplemented by analysis of a data subset from which highly organic samples are excluded (Model 2). Model 2 is run with and without particle size data (Models 2a and 2b respectively). Finally, to address concerns that the impact of some environmental factors such as *MAR* is masked by effects of waterlogging, multiple regression is also applied to the Model 2b data subset after having removed all but the best drained (Class 4) samples (Model 3). Thus, Model 3 tests, for example, whether stronger linear relationships exist between *logMAR* and soil magnetism in free-draining soils. Multiple regression analyses are carried out for χ_{LF} and χ_{FD} % but not mass specific χ_{FD} as this parameter shows a close correspondence to χ_{LF} in the England and Wales dataset (Figure 3f).

Zero order correlations

For Model 1, and for both χ_{LF} and χ_{FD} %, *Parent Material* is the highest ranked factor with 23 - 25 % explanation of variance, followed by *Drainage* with 14 – 19 %. (Table 8). Of the remaining variables used only four (*Land use, Texture, logMAR* and *Slope*) account for ≥ 5 % variation in any magnetic parameter. However, χ_{LF} and χ_{FD} % show very different environmental associations: *Land use* and *Texture* are important explanatory factors for χ_{LF}, while *Slope* and *MAR* are substantially more powerful explanatory factors for χ_{FD} % (Table 8). When categorised, (Supplementary Information Table 1) the nonlinear variables associated with organic rich soil and peat appear to be more influential factors upon χ_{LF}. However, the majority of variance is still accounted for by *Parent material*, *Drainage*, *Land use* and *Texture*.

With highly organic samples excluded (Model 2a), there is less difference between χ_{LF} and χ_{FD}% with *MAR* becoming the third ranked factor (after *Parent material* and *Drainage*) for both parameters (Table 10a - b). This change from Model 1 is explained by the influence of high rainfall peat-rich sites included in the full sample set. Lower ranked factors are also not very different between χ_{LF} and χ_{FD}%. Although the ranking shows slight differences, the amounts of variance explained are similar in all cases, and far lower than the top three factors. The similarity of χ_{LF} and χ_{FD}% in their relationships to environmental factors is not affected by the inclusion of particle size data (Model 2b). For both parameters *CSand* is second only to *Parent material* as a univariate explanatory factor. Exclusion of poorly drained samples (Model 3) has little impact on the higher ranked factors, but does markedly increase the fraction of χ_{LF} variance explained by *logMAR*.

Multivariate regression analysis

Standard multiple regression analysis is carried out on the same datasets (Models 1, 2a, 2b and 3) to determine the level of explanation that can be achieved with regard to logχ_{LF} and χ_{FD}%, and to estimate the unique contribution of each environmental factor. Further statistics and figures examining, possible univariate and multivariate outliers are considered in the Supplementary Information.

Model 1 for logχ_{LF} (Table 9a) shows r is significantly different from zero, $F(11, 4884) = 283.27$, $p < 0.001$, giving an adjusted r^2 of 0.39. As measured by the partial and part (see definitions in Supplementary Information) r^2 values and beta coefficients, the most significant contributors are *Parent material*, *Drainage*, and *Land use*. If used together without the other factors, *Parent material* and *Drainage* produce a model with r^2 of 0.29

and RMSE of 0.40. At the $p < 0.001$ significance level variables *Time*, *logrMAT* and *logSlope* are not significant contributors to the model prediction. Model 1 for χ_{FD} % gives an adjusted r^2 of 0.36. In common with χ_{LF}, *Parent material* and *Drainage* are the most important variables as signified by the largest beta coefficients and account for the greatest unique variance in χ_{FD} % when all other factors are accounted for (Table 9b). *Texture*, *Land use* and *logOC* have less predictive power than for $\log\chi_{LF}$, but *logMAR* has greater importance. These differences in the position of lower ranking factors are probably due to the loss of peat-based samples in the frequency dependent data set that reduces the number of sites with very high rainfall and upland land uses.

Model 2a (Table 10 a - b), as with Model 1, employs standard multiple regression and all variables to predict both $\log\chi_{LF}$ and χ_{FD} %. Model 2a for $\log\chi_{LF}$ shows r significantly different from zero, $F(11, 4332) = 261.27$, $p < 0.001$, giving an adjusted r^2 of 0.40 and a lower RMSE of 0.333. *Parent material* has the greatest partial and part r^2 values, with *Drainage* as the second most important factor. Only two other factors have partial r^2 values of greater than 0.02; *Texture* and *Land use*. In contrast to the zero order correlation, the partial and part r^2 values for *MAR* are very low, suggesting that *MAR* has little unique influence over $\log\chi_{LF}$. If *Parent material* and *logMAR* are used alone in a standard multiple regression for $\log\chi_{LF}$ only 1.8 units of the 28 % variance accounted for by the total model are unique to *logMAR* despite a zero order correlation of 0.07, suggesting most of the shared variance can be attributed to *Parent material*. The partial r^2 and zero order correlation values for *Land use* are also far lower than for Model 1, demonstrating that the relationship between *Land use* and $\log\chi_{LF}$ in Model 1 is largely due to the effects of peat-based soils with little variation attributable to other land use categories. The variables of *logSlope*, *Time* and *logAlt* have the weakest unique contributions to the model. Model 2a for χ_{FD} % derives r significantly different from zero *F*(11, 4258) = 228.11, $p < 0.001$, giving an adjusted r^2 of 0.37 and a RMSE of 2.20. Compared with Model 1 for χ_{FD} %, *Parent material, pH* and *Drainage* strengthen as unique contributors, while*, logSlope, Texture, Time* and *Land use* decline. *LogMAR*, despite increasing in zero order correlation, shows only a minor increase in partial r^2. All factors change relatively little as a result of removing samples with 'unreliable' χ_{FD} %, values, equivalent to removing samples with %OC > 12.

Model 2b for logχ_{LF}, r differs significantly from zero, *F*(12, 4116 df) = 282.41, $p < 0.001$, giving an adjusted r^2 of 0.45 and a RMSE of 0.319 (Table 10c), with *CSand* making a substantial contribution, with partial, part and zero order r^2 values second only to *Parent material*, with the contributions of all other factors except *Texture* weakening with their addition. The unique impact of *logMAR*, already small for Model 2a (r^2 = 0.011), declines substantially in Model 2b (r^2 = 0.003). For χ_{FD} %, model 2b has an r value that differs significantly from zero for Model 2b *F*(12, 4048 df) = 220.40, $p < 0.001$, giving an adjusted r^2 of 0.40 and a RMSE of 2.17 (Table 10d). A weakening of the unique impacts of *Parent material* and *Drainage* is evident, as the factor of *logCSand* shares some of these factors with previously unique accounted variance. *logCSand* now ranks as the third greatest unique contributor (partial and part r^2), but in isolation has the second highest zero order r^2. As with logχ_{LF}, *Texture* becomes slightly more important, while *logMAR* makes a similar small unique contribution.

Model 3 for logχ_{LF} has r significantly different from zero, *F*(11, 2035) = 157.963, $p <$ 0.001, giving an adjusted r^2 of 0.46 and a relatively low RMSE of 0.331 (Table 11a). The effects of removing both poorly drained and high organic carbon soils are most obvious for *Parent material* and *logCSand* which have substantially greater zero order and partial r^2 values. *Texture* is the next most substantial unique contributor, with the remaining factors accounting for very minor amounts of unique variance. Zero order correlation declines for *logSlope* as samples from poorly drained areas are removed reflecting low slope angles, but its unique contribution remains extremely low. As with Model 2b, *logMAR* has very little unique impact, despite its relatively large zero-order contribution. This implies, as in Model 2, that virtually all of the variance explained by *logMAR* in the zero order correlation is shared with *Parent material*. Model 3 for lχ_{FD} % has r significantly different from zero, $F(11, 2025) = 111.127$, $p < 0.001$, giving an adjusted r^2 of 0.37 and RMSE of 2.16 (Table 11b). The first two ranked contributors (disregarding the excluded *Drainage*) are unchanged but now exhibit strengthened contributions (Table 11a-b). As with logχ_{LF} , *logMAR* is elevated to the third most important contributor to the regression as judged by zero order correlations. However, as the part correlation shows when using accounting for the effect of other all variables, *logMAR* only accounts for 0.5 units of the total explained variance of 37 %. Importantly, despite low unique contributions, zero order correlations for *LOC* and *Time* increase appreciably for Model 3, and as with logχ_{LF}, the zero order correlation for *logSlope* declines.

<u>6.0 Discussion</u>

6.1 Magnetism and soil factors

Parent material

Both bivariate and multivariate analyses place *Parent material* as the factor with the highest level of explanation at this spatial scale of analysis, reaffirming the ranking of parent material as a first order control in the conceptual model (Figure 1). The mean magnetic value for each *Parent Material* explains a high proportion of variance in both magnetic parameters (typically ~23 – 33 % depending on applied constraints). Importantly, *Parent material* also accounts for the most unique variance in all models. Mean magnetic values for *Parent material* are positively correlated with mean magnetic values (employing model 1 dataset) for *Drainage* (r = 0.3), *Texture* (r = 0.23), *logSlope* (r = 0.27) and values of *logMAR* (r = 0.23).

As noted above (sections 2.1 and 2.2), previous studies of soils across England and Wales (Tite, 1972, Dearing et al., 1996a) show that high χ_{LF} values are often linked with elevated Fe concentrations, such as in soils overlying *Limestone ooidal* (Jurassic) and *Schist* or *Slate*. Indeed, if extreme outliers (n = 81) mostly due to ferruginous parent materials are removed (untransformed Fe may then be employed) from the reduced subset, total soil Fe (mg kg^{-1}) shows a high correlation with $\log\chi_{LF}$ ($r^2 = 0.30$, $p < 0.05$) and less positive but still significant correlations with frequency dependent data (Figure 10; Table 12). The mean √ Fe concentration for soils (using all data) on particular parent materials also shows a positive gradient (Figure 11). This is consistent with the proposed causal links between parent material, soil Fe concentrations and SFM formation (Dearing et al., 1996a).

However, not all samples with elevated √ Fe have increased $\log\chi_{LF}$ values as shown by soils developed upon *Mudstone (M), Mud-rich Limestone*, *Limestone impure*, *Halitic rocks* and *Tidal flat* (Figure 11 a). In these situations, it could be argued that SFM formation is not favoured due to adverse pedogenic conditions. Conversely, it is possible to observe relatively low total Fe concentrations associated with moderately high χ_{LF}

values as demonstrated by the mean logχ_{LF} values for soils on parent materials such as *Chalk*, *Sandstone (P), Granite*, and *Glaciofluvial deposits*. Mean χ_{FD}% values are also strongly associated with total Fe and show a similar relationship (Figure 11 b), but low values for *Alluvium*, despite relatively high mean √ Fe, suggest a further a link with drainage.

Climate

In the conceptual model (Figure 1), climate is postulated as a first order control on soil magnetism. In this study, however, the associations between *MAR* and *MAT* and magnetic parameters are relatively weak. Model 1, demonstrates that *logMAR* shows no significant linear relationship with logχ_{LF}. However, by restricting samples to *%OC* < 12, a large increase in zero order r^2 demonstrates its greater ability to predict logχ_{LF} and χ_{FD} % despite accounting for very little unique variance when used with the other factors. Similarly, the effect of *logMAR* is complicated by differences in *Parent material* and *Drainage* factors. If samples affected by poor drainage are removed, as in model 3 (Figure 12a and c), the relationship with *logMAR* strengthens. By restricting the dataset further to samples that have *MAR* values < 1500 mm a stronger relationship is evident. If the dataset in Model 3 is constrained for *Parent material* the relationship between *logMAR* and logχ_{LF} for a particular parent material is often one of increasing χ_{LF} up to *logMAR* ~1200 - 1500 mm followed by a decline (Figure 13). However, given the importance of Fe as driver of SFM production, any positive correlation with *logMAR* (Model 3) may well be coincidental as the wettest areas in England and Wales tend to have the more Fe-rich parent materials.

It has been suggested by Maher and Thompson (1995) that above 1500 mm rainfall soil conditions become adverse for pedogenic magnetic enhancement, a finding that is largely supported here. After removing the effect of parent material there appears to be a small positive influence from *logMAR*. This may reaffirm the link between rainfall and weathering, but strong bivariate correlations with organic carbon and pH may also point to additional roles in magnetic enhancement processes. In contrast to rainfall, the role of temperature in controlling the magnetic dataset is small: *logrMAT*, both in the constricted and whole data sets, shows little relationship with soil magnetism. This suggests that any effect, if it exists, operates at a continental scale.

Relief and Drainage

Relief and drainage are viewed in the conceptual model as second order factors, operating at more local scales. Although there are significant associations between *logSlope* and the magnetic parameters (Supplementary Information, Figure S4), the effects of relief, as encapsulated by *logSlope* and *logAlt*, are relatively weak when all data are considered (Model 1). Steeper slope angles (especially > 12°) are more often associated with good drainage and many of these soils are upon parent materials with soils exhibiting higher magnetic values, but they represent only a minority of samples. Generally *logSlope*, except at relatively high values, gives little insight into levels of drainage in the soil and rarely accounts for additional variance beyond that explained by *Parent material* alone. Relief is therefore an influential factor on soil magnetism through its inter-correlations with others factors; the relevance of altitude and slope being realised at their upper extremes. High altitude areas, for example, exhibit high rainfall and often peaty soils. Steeper slopes, although coincident with greater rainfall are better drained and generally associated with parent materials that in this dataset exhibit soils with greater magnetic values. The clear separation of magnetic values, especially χ_{FD} %

(Table 2), for the similar parent materials *Sandstone and Mudstone (P)* and *Sandstone and Mudstone (M),* the former on average associated with steeper and better drained slopes (*logSlope* $\overline{x}$ = 0.85 ± 0.07 and $\overline{x}$ = 0.62 ± 0.1, respectively), suggests that slope may have a stronger effect at sub-regional scales.

The effect of drainage is explored though the use of *Texture* and *Drainage* categories. *Texture* is inter-correlated with *Parent material*, *Land use*, *pH*, *OC* and *MAR*, as exemplified by the partial correlation between *Texture* and $\log\chi_{LF}$ of r = 0.15 (r^2 = 0.02) after all other variables are held constant. However, it retains a significant level of explanation even after parent material is accounted for.

Drainage index ranks second to *Parent material* when all data are employed for both zero order and partial/part correlations with magnetic parameters (Table 9a-b), but the strength of correlation between these variables is relatively low (r = 0.30, $p < 0.05$) suggesting some degree of independence. A multiple regression model with only *Parent material* and *Drainage* as variables is able to account for 29 % (total with all variables is 39 %) and 31.8 % (total with all variables is 36 %) of the variability in $\log\chi_{LF}$ and χ_{FD} % respectively, with only 9 % and 16 % common shared explained variance. However, *Drainage* is relegated to third position when *CSand* is included in Model 2b. The importance of *CSand* underlines the positive role of free drainage, providing a more discriminatory variable of drainage than the broad and qualitative drainage classes. The significance .of *CSand* might be interpreted in terms of a proxy for primary minerals. However primary minerals (especially primary magnetite) tend to fall into a silt sized fraction (2 - 63 µm) with which there is no correlation. Also, there are no significant associations between *CSand* and parent materials expected to contain primary magnetic minerals, and such an interpretation would contradict the high correlations between *CSand* and χ_{FD} values.

Figure 14 demonstrates graphically the link between parent material, drainage and soil magnetism. *Parent materials* ranked according to the frequency of soils with drainage class 4 (free-draining) show a corresponding declining trend in mean χ_{LF} and χ_{FD} % values. Some *Parent material* categories show mean magnetic values that lie consistently above the trend: *Limestone (Ooidal), Schist and slate, Mudstone (P) and Mudstone and Sandstone (P).* These are all Fe rich and highly weatherable substrates. This is consistent with the conceptual model that predicts the weathering of Fe and the existence of free-draining soil profiles compound their individual effects to cause the highest rates of SFM production and accumulation.

Organisms and Vegetation

Organisms and vegetation are considered in the conceptual model (Figure 1) as second or third order factors whose effects operate most strongly at local scales. This idea is supported by the relatively low rankings of *Land use*, *%OC* and *pH* for explaining overall variability in magnetic parameters. For bivariate analyses (Table 8), *Land use* is the highest ranked for all three parameters and, in terms of land use type, *ley grassland* is the highest ranked (Table 5b). However, the regression analysis shows that the level of explanation is confounded by the presence of many soils with high levels of organic carbon. The results of regression Model 2a demonstrate that the relationship between

Land use and $\log\chi_{LF}$ is largely due to the effects of peat-based soils with little variation explained by *Land use* when they are excluded from the analysis.

The association of *logOC* with magnetic parameters (See Supplementary Information Figure S7; Table 6a) shows the greatest positive correlation in samples with *%OC* < 5.4 %. Low to moderate levels of organic carbon suggest a relatively fast carbon turnover characteristic of a biologically active system. An assumption that %OC represents organic substrate availability for bacterial activity in the rhizosphere is consistent with arguments for the need for populations of DIRBs to expand during anaerobic episodes. The linear relationship between *%OC* and magnetic parameters suggests that %OC may even represent limiting conditions up to a threshold value of ~ 6 %. Above this level, the accumulation of large amounts of organic matter driven by poor drainage, low temperature and acidic conditions might represent soil conditions inimical to bacterially mediated SFM formation or accumulation.

Overall the explanatory power of *pH* is low, due to bimodal associations with all three magnetic parameters (See Supplementary Information, Figure 8). *pH* is also strongly correlated with *Land use* and *logMAR* ($r = 0.53$ and -0.60, $p < 0.05$) and Models 2 and 3 show that *pH* has low explanatory power even when samples from the organic and wet uplands are excluded. Thus, it seems that *pH* is strongly dependent on other factors at this scale although it may be an important contributor to iron transformation processes and SFM formation at more localised scales.

Assessment of organisms and vegetation is complicated by studying areas with a millennial-scale history of forest clearance and land use change, which includes the use of fire, introduction of agricultural methods and application of manures and soil conditioners. In fact, it is doubtful whether the variability in *%OC* and *pH* in lowland soils 7000 years ago would have been as high under continuous forest cover as it is today. It could therefore be argued that the presence of strong associations in the modern environment indicate that soil magnetic properties have tracked changing soil conditions. The evidence here for controls on SFM formation by *%OC* and to a lesser extent *pH*, rather than *Land Use* itself, suggest that soil chemistry, rather than broader land management scenarios, are important drivers for local variations in soil magnetic properties.

Time

Time in pedogenesis is probably the most intractable factor. The previous discussion suggests that magnetic properties may be in equilibrium with modern soil conditions, but can we identify longer term controls? A simple comparison across 3 areas (Table 7) shows no significant associations between time elapsed for pedogenesis and magnetic properties, and multiple regression Model 1 shows *Time* with statistically significant but low explanatory power (Table 9). However, Model 3 (Table 11) shows that the factor of *Time* displays an increased zero order correlation for lχ_{FD}%.

One problem in these analyses is the confounding effects of parent material that is not equally represented in each area. Figures 15 (a – f) demonstrate the importance of parent material between areas through the ability of the mean magnetic value for soils developed upon different parent materials to predict the actual magnetic value. It can be seen that r^2 values increase when predicting both logχ_{LF} and χ_{FD}% from Area 1 to 3 as *Parent material* loses explanatory power. In order to control for the effect of *Parent Material*, an analysis was undertaken of samples that span all three areas on *Chalk.* To minimise further differences in soil attributes 'arable' *Land use* and dominant soil sub groups 3.41-3.43 (Humic rendzina, Grey rendzina, and Brown rendzina) were selected. Climate differences across all the *Chalk* areas are small and ignored in the analysis. ANOVA test results suggest that there are no statistically significant differences between means for logχ_{LF} across all three areas, irrespective of the constraints for soil type and land use. In contrast means of χ_{FD} % show significant differences between areas for all constraint options (all samples on *Chalk*, Welch $F(2, 47.33\text{df}) = 10.25$, $p < 0.05$; dominant soil type, Welch $F(2, 11.52\text{df}) = 13.86$, $p < 0.05$; arable land use, Welch $F(2, 6.965\text{df}) = 10.57$, $p < 0.05$). Games-Howell *post-hoc* tests indicate that Area 1 and 2 have significantly different means for all samples, whereas Areas 1 and 2, and 3 and 1 have significant differences when constrained by land use and soil type.

Thus, these results suggest that the concentration of ferrimagnetic grains is not a direct function of pedogenic time over timescales spanning the late Pleistocene. However, higher χ_{FD} % values in chalk soils in Area 1 compared to Area 2 and specifically, at the further constraining levels, between Area 1 and Area 2, and between Area 2 and Area 3 provide significant evidence for a shift in the ferrimagnetic grain distribution, with the proportion of VSPM grains to all ferrimagnetic grains increasing with age. It is not possible to identify whether this effect is common across different parent materials or specific to chalk. If specific to chalk, one plausible explanation would be a shift in the ferrimagnetic grain size distribution through time as VSPM grains accumulate in the presence of SD magnetic inclusions (Hounslow and Maher 1996).

Unexplained factorial variance

The multiple regression models account for 36 – 46 % of variance in the two magnetic parameters and there are several potential causes for the unexplained variance. First, there are several sources of error and variability. These include compositional categories (eg. parent materials) that are not ideally constrained, differences between the scale of some data sets (eg. geological classes taken from Digimap), the inherent large scale variation found in many soil properties at the field scale, and random ferrous materials introduced to the soil system, such as metallic and minerogenic trash, which are not excluded by the criteria used for polluted soils. Second, the contribution by weakly magnetic Fe-bearing paramagnetic minerals increases disproportionately in soils with low χ_{LF} values. Third, the concentration of ferrimagnetic minerals in a sample is diluted by the presence of diamagnetic (non-magnetic) materials, such as calcium carbonate and organic matter. This can be expected to suppress χ_{LF} and χ_{FD} values in, particularly, chalk and peat soils though the quantitative effects are estimated not to be significant to the overall patterns. Fourth, there are potentially different sets of conditions driving the production of ferrimagnetic minerals that are not easily simulated in this study. For example, the cluster of high χ_{LF} and χ_{FD} values south of The Wash in eastern England (Figure 4) not associated with Fe-rich parent materials is a potential anomaly. This cluster of over 30 samples has an environmental context quite different from other highly magnetic clusters as it is situated at the edge of peatlands over marine sediments. One plausible explanation that is currently under examination is the formation of greigite (Fe_3S_4), a ferrimagnetic iron sulphide produced under anaerobic conditions in the presence of sulphur-containing sediments and sulphate-reducing bacteria.

Overall the ranking of factors is overwhelmingly dominated by parent material and drainage, including the significant variable of coarse sand. A second group of influential but subordinate factors includes mean annual rainfall, slope and altitude, land use, organic carbon and pH. A third group of factors including mean annual temperature and time are deemed not relevant at these spatial and temporal scales.

6.2 SFM formation

SFMs and soil types

Findings here are highly consistent with the ranking of soil groups and sub groups (Table 13) by mean magnetic values. Soil classification in England and Wales takes into account a range of factors that are instrumental in the formation of a particular soil. Excluding man-made soils, Lithomorphic, Podzolic and Brown Soils are the three highest ranked major soil groups in all three magnetic parameters. Typical Brown Podzolic, Brown Ranker and Brown Rendzina are in the top three positions for all magnetic parameters in the ranking of soil sub-groups. By contrast, the lowest ranked major soil groups for all parameters are Terrestrial Raw, Raw Gley and Groundwater Gleys, and for soil sub-groups the lowest positions are dominated by categories such as Stagnogley Podzol, Typical Humic Gley, Raw Oligo-fibrous Peat, Typical Sandy Gley, Pelo-Calcareous Alluvial Gley and Cambic Stagnohumic Gley. All these soil types utilise classification criteria that are strongly linked to parent material type and drainage. The dominant factor in these rankings appears to be drainage, with well-drained soils ranked high and poorly drained soils (eg. gleys) ranked low. However, while Typical Brown Podzolics are ranked first, other true podzols (eg. Humo-Ferric Podzol) are ranked much lower suggesting that free drainage that promote incipient podzolisation is positive with regards SFM formation, but extreme chelation and eluviation are destructive. Parent material plays a significant role in identifying young and thin soils (rankers) and lithomorphic rendzina soils on calcareous substrates, both ranked highly. The strength of association between soil sub groups and soil magnetism may be gauged by plotting actual observed magnetic values against mean values for each soil sub-group (Figure 16). The correlation coefficients (figure 16) are similar or better than explanations using Model 1 (r^2 values (0.37 - 0.38) showing that the combination of factors inherent in soil classification are a strong predictor of soil magnetic properties.

SFM concentrations and distributions

One remarkable finding in the study is the strength of magnetic inter-parameter correlations (Figure 3). These are partly explained by interrelated expressions, yet for the majority of non-polluted samples measured the data suggest (Figure 3f) that the concentration of VSPM grains (χ_{FD}) is directly proportional to the total concentration of ferrimagnetic minerals (χ_{LF}). The weaker relationship between the total ferrimagnetic concentration (χ_{LF}) and the distribution of ferrimagnetic grains (χ_{FD} %) indicates (Figure 3b) that the highest categories of χ_{FD} % (10 - 14 %) effectively define an 'ultimate' grain size distribution where the proportion of VSPM grains to the combined total of smaller and larger SP, PSD, SD and MD grains is maximal. Thus, a key question to ask is why other soils fail to reach this level of χ_{FD} %. There are several possible reasons: 1) processes involving abiotic aging of ferrihydrite to maghemite (cf. Barrón and Torrent 2002) or magnetite crystal growth (e.g. Hansel et al., 2003) may be expected to produce more SD grains which suppress χ_{FD} %; 2) the balance between formation/accumulation and destructive processes may be skewed towards destruction, such that the population of the finest grains including VSPM is constrained; 3) the SFM mechanism varies in terms of the grain size distribution formed depending on local soil conditions.

SFM conceptual model

The findings from the study essentially confirm the SFM conceptual model as it applies to temperate regions (Figure 1) but with qualifications. Parent material remains the first order control operating at regional scales providing the source of Fe through weathering for SFM production. All other factors being equal, it seems that parent materials that are either deficient in Fe-bearing minerals or typified by very slow rates of weathering will not produce a rate of Fe supply that is conducive to the production and accumulation of high concentrations of SFMs. The equally important drainage factor means that good drainage in surface soils provides the essential anoxic-oxic cycling in the microenvironment as the soil changes from wet to dry conditions. Poorly drained soils lack oxic phases and maximise the effects of reductive diagenesis. The subordinate but positive effect of mean annual rainfall suggests that Fe-supply is at least partly driven by the intensity of hydrolysis. Thus for England and Wales, at least, we may speculate that there are two critical stages in the process of SFM production and accumulation that involve initially the supply of Fe and secondly the presence of free drainage. These stages are consistent with both the ferrihydrite-maghemite-hematite (Barrón and Torrent 2002) and ferrihydrite-magnetite (maghemite) (Dearing et al., 1996a) models. However, the subordinate role of climate largely through rainfall rather than temperature would argue strongly for the ferrihydrite-magnetite (maghemite) process to be dominant in temperate regions, particularly as the ferrihydrite-maghemite-hematite process is strongly temperature sensitive. Additionally, the weak association of low to moderate levels of organic carbon and pH with optimal distributions of nanoscale VSPM grains may indicate a minor contribution of DIRB reduction of ferrihydrite to magnetite formation. However, the evidence does not support a major contribution of biotic processes to what is dominantly an abiotic steady state mineral transformation. Further ongoing studies will assess the roles of soil forming factors operating at local spatial scales (< 5 km) and short timescales (<103 years) and seek to confirm the biogeochemical soil processes that drive magnetic mineral formation and destruction under different climatic regimes.

7.0 Conclusions

A comprehensive analysis of soil factors and three magnetic susceptibility parameters in surface soils across England and Wales at a spatial resolution of 5 x 5 km shows that the importance of factors is broadly: 1) parent material and drainage; 2) mean annual rainfall, slope and altitude, land use, organic carbon and pH. Mean annual temperature and time (>10^3 years) do not appear to be significant factors at these spatial and temporal scales. About 11% of the samples, mainly from areas close to urban and older industrial centres, are considered contaminated by atmospheric pollution particles.

Multiple regression models show that soil forming factors account for 36 - 46 % of variance in the two magnetic parameters, with parent material and good drainage together accounting for ~ 30 % of the magnetic variability in the complete dataset. A surprising and potentially important finding is the relevance of coarse sand which is second only to parent material as an explanatory factor of soil magnetic values, underlining the importance of soil drainage.

The results are consistent with a dominant mechanism of SFM production driven by Fe-supply from weathering, followed by the production of ferrihydrite with conversion to magnetite/maghemite minerals within the SP and SSD grain size ranges. The importance of organic carbon and pH suggests that biomineralization through bacteria mediated Fe reduction may play an additional role in the production of SFMs.

Figure captions

Figure 1. Proposed sequence for secondary ferrimagnetic mineral formation in temperate soils from Dearing et al. (1996a), showing main Fe phases (upper case lettering), important processes (lower case lettering) and factors (bold lettering) at different stages. The possible weathering of metastable SFMs is shown as a dotted line.

Figure 2. Relationship between the magnitude of $\kappa_{LF} \times 10^{-5}$ and the uncertainty of calculated κ_{FD} % values (10 $\kappa_{LF} \times 10^{-5}$ is approximate to 0.1 $\chi_{LF} \times 10^{-6}$ m^3 kg^{-1} here based on approximately 10 gram samples)

Figure 3. Scatter plots of a) χ_{FD}% vs logχ_{LF} b) χ_{FD}% vs χ_{LF}, c) χ_{FD}% vs logχ_{FD} , d) χ_{FD}% vs χ_{FD} e) log χ_{FD} vs log χ_{LF} f) χ_{FD} vs χ_{LF}. Grey points represent those samples that are within the 'polluted' sample thresholds. Linear regressions shown exclude polluted samples. Subtract 1 for true values on the log scale for χ_{FD} as this is subject to a 'started' transformation.

Figure 4. Spatial patterns of topsoil magnetic properties at 5 × 5 km resolution across England and Wales: a) placenames and geographical features; b) χ_{LF} ; c) χ_{FD} : d) χ_{FD}%. Regions mentioned in the text: 1) Cheviot Hills; 2) Pennines; 3) Yorkshire Wolds; 4) Lincolnshire Wolds; 5) Malvern Hills; 6) Cotswold Hills; 7) Cambridgeshire/Lincolnshire Fens; 8) Chiltern Hills; 9) Berkshire Downs; 10) Salisbury Plain; 11) Somerset Levels; 12) Exmoor; 13) Dartmoor; 14) North Downs; 15) Wealden Hills; 16) South Downs; 17) New Forest National Park; 18) South Wales Mining Valleys. Ice sheet limits (Fig 4a)

have been derived using glacial advance maps derived from Bowen et al. (1986) and later evidence from the BRITICE map and GIS database (Clark et al., 2004)

Figure 5. Spatial distribution of magnetically polluted topsoil samples at 5 x 5 km resolution across England and Wales. Urban areas are shaded in grey.

Figure 6. Spatial distribution of a) bedrock and b) superficial geology (as aggregated for this study) and c) soil major group for each data point in the complete dataset.

Figure 7. Scatter plots of mean magnetic values for each *Parent material* category versus individual sample values: a) logχ_{LF}, b) logχ_{FD} and c) χ_{FD} %. Subtract 1 for true values on the log scale (second y axis) for χ_{FD} (fig 7b) as this is subject to a 'started' transformation.

Figure 8. Box plots of sample magnetic values for *Drainage* classes: a) logχ_{LF}, b) logχ_{FD} and c) χ_{FD} %. Subtract 1 for true values on the log scale (second y axis) for χ_{FD} (fig 8b) as this is subject to a 'started' transformation. White and black horizontal lines within the box represent the mean and median respectively. Upper and lower box boundaries represent 75th and 25th percentiles and upper and lower whiskers denote the 90th and 10th percentiles. Crosses represent outlying values.

Figure 9. Scatter plots of sample χ_{LF} values versus % *Particle size* for classes clay (< 2 μm), silt (2 - 63 μm), very fine sand (63 - 125 μm), medium fine sand (125 - 250 μm), medium sand (250-500 μm) and coarse sand (500 - 2000 μm)

Figure 10. Scatter plots of sample magnetic values versus total Fe *:* a) logχ_{LF}, b) logχ_{FD} and c) χ_{FD} %. The solid black line represents a linear regression fit. Box plots of same data based on classes detailed in Table 12: d) logχ_{LF}, e) logχ_{FD} and f) χ_{FD} %. Subtract 1 for true values on the log scale (second y axis) for χ_{FD} (fig 10b and e) as this is subject to a 'started' transformation.

Figure 11. Scatter plots of sample magnetic values versus mean √ Fe for specific *Parent materials* (where n > 20) with accompanying error bars denoting ±1 standard deviation: a) logχ_{LF}, b) as a) for χ_{FD} %. Line plots represent the mean magnetic values for each parent material.

Figure 12. Scatter plots of logχ_{LF} against *Mean annual rainfall* (*logMAR):* a) samples with drainage class 4 and %OC < 12, and b) with the added constriction of no samples with *MAR* > 1500 mm. Figures 12 c - d as above for χ_{FD} % values.

Figure 13. Scatterplots of logχ_{LF} versus *logMAR* for selected parent materials: for data within Model 3. Dashed lines denote rainfall of 1200 mm where a general peak in the maximum magnetic parameter value is observed.

Figure 14. Column charts displaying % of each drainage class for soils associated with *Parent material* types (where n > 20): a) line plot represents the mean logχ_{LF} for each parent material; b) as a) but for χ_{FD} %. For *Drainage*, grey represents class 1, cross-hatching class 2, hatching class 3 and clear class 4.

Figure 15. Scatter plots of mean logχ_{LF} for parent material values versus individual sample values for each *Time area*: a) Area 1, b) Area 2, and c) Area 3.

Figure 16. Scatter plots of mean magnetic values for each soil subgroup classification versus individual sample values: a) logχ_{LF}, b) logχ_{FD} and c) χ_{FD} %. Subtract 1 for true values on the log scale (second y axis) for χ_{FD} (fig 16b) as this is subject to a 'started' transformation.

Table captions

Table 1. Summary statistics for the complete and reduced (excluding polluted samples) magnetic data set for χ_{LF}, χ_{FD} and χ_{FD} % values.

Table 2. Top 10 and bottom 10 ranked *Parent materials* categories, based on mean logχ_{LF}, logχ_{FD} and χ_{FD} % values for associated soil samples. Only parent material categories with > 20 occurrences are displayed.

Table 3. Mean logχ_{LF}, logχ_{FD} and χ_{FD} % values for *Mean annual rainfall* (*MAR)* and *Mean annual temperature* (*MAT)* classes.

Table 4. Mean logχ_{LF}, logχ_{FD} and χ_{FD} % values for a) *Altitude* (classes based on percentiles), b) Slope angle and c) Drainage classes..

Table 5. Mean logχ_{LF}, logχ_{FD} and χ_{FD} % values for a) soil *Texture* and b) *Land use* categories.

Table 6. Mean logχ_{LF}, logχ_{FD} and χ_{FD} % values for a) *%OC* (based on percentiles) classes and b) pH classes.

Table 7. Mean logχ_{LF}, logχ_{FD} and χ_{FD} % values for soils in Areas 1 - 3 (Time factor).

Table 8. Correlation coefficients (r) and coefficients of determination (r^2) in brackets of all variables selected to represent soil forming factors of Jenny's equation. Variable values

are either based on category means or transformed/raw data values as ascribed in the results text. N/S = not significant $p < 0.05$, * = not significant $p < 0.01$.

Table 9. Simultaneous multiple regression output for a) logχ_{LF} and b) χ_{FD}% using all variables (Model 1). Zero order, partial and part correlations are displayed together with regression coefficients (unstandardized and standardized, *B* and beta), *t* statistic and level of significance.

Table 10. Simultaneous multiple regression output for a) logχ_{LF} and b) χ_{FD}% (Model 2a without *CSand*); c) logχ_{LF} and d) χ_{FD}% (Model 2b with *CSand*). Zero order, partial and part correlations are displayed together with regression coefficients (unstandardized and standardized, *B* and beta), *t* statistic and level of significance.

Table 11. Simultaneous multiple regression output for a) logχ_{LF} and b) χ_{FD}% using all variables (Model 3). Zero order, partial and part correlations are displayed together with regression coefficients (unstandardized and standardized, *B* and beta), *t* statistic and level of significance.

Table 12. Mean logχ_{LF}, logχ_{FD} and χ_{FD}% values for Fe categories.

Table 13. Mean logχ_{LF}, logχ_{FD} and χ_{FD}% values for a) major soil groups and b) soil subgroups.

References

Avery, B.E., Bascomb, C.L., 1974. Soil survey laboratory methods. Soil Survey technical monograph no. 6. Soil Survey of England and Wales, Harpenden pp83.

Barrón, V., Torrent, J., 2002. Evidence for a simple pathway to maghemite in Earth and Mars soil. Geochimica et Cosmochimica Acta 66 : 2801-2806.

Barrón, V., Torrent, J., De Grave, E., 2003. Hydromaghemite, an intermediate in the hydrothermal transformation of 2-line ferrihydrite into hematite. American Mineralogist 88: 1679–1688.

Bityukova, L., Scholger,R., Birke, M., 1999. Magnetic susceptibility as indicator of environmental pollution of soils in Tallin. Physics and Chemistry of the Earth Part a-Solid Earth and Geodesy 24: 829-835.

Blake, W.H., Wallbrink, P.J., Doerr, S.H., Shakesby, R.A., Humphreys, G.S., 2006. Magnetic enhancement in wildfire-affected soil and its potential for sediment-source ascription. Earth Processes and Landforms 31: 249-264.

Bloemendal, J., Lamb, B., King, J., 1988. Paleoenvironmental implications of rock - magnetic properties of Late Quaternary sediment cores from the eastern equatorial Atlantic. Paleoceanography 3: 61-87.

Bowen, D.Q., Rose, J., McCabe, A.M., Sutherland, D.G., 1986. Correlation of Quaternary glaciations in England, Ireland, Scotland and Wales. Quaternary Science

Reviews 5: 299-340.

Boyko, T., Scholger, R., Stanjek, H., 2004. Topsoil magnetic susceptibility mapping as a tool for pollution monitoring: repeatability of in situ measurements. Journal of Applied Geophysics 55: 249-259.

Clark, C.D., Evans, D.J.A., Khatwa, A., Bradwell, T., Jordan, C.J., Marsh, S.H., Mitchell, W.A. and Bateman, M.D., 2004. Map and GIS database of landforms and features related to the last British Ice Sheet. Boreas 33: 359-375.

Dalan, R.A., Banerjee, S.K., 1996. Soil magnetism: an approach for examining archaeological landscapes. Geophysical Research Letters 23: 185-188.

Dearing, J.A., 1999. Holocene environmental change from magnetic proxies in lake sediments. In: B.A. Maher, R, Thompson (Editors), Quaternary Climates, Environments and Magnetism. Cambridge University Press, Cambridge, pp. 231-278.

Dearing, J.A., 2000. Natural magnetic tracers in fluvial geomorphology. In: I.D.L. Foster, (Editor), Tracers in Geomorphology, Wiley, Chichester, pp. 57-82.

Dearing, J.A., Bird, P.M., Dann, R.J.L., Benjamin, S.F., 1997. Secondary ferrimagnetic minerals in Welsh soils: a comparison of mineral magnetic detection methods and implications for mineral formation. Geophysical Journal International, 130: 727-736.

Dearing, J.A., Dann, R.J.L., Hay, K., Lees, J.A., Loveland, P.J., Maher, B.A., O' Grady, K., 1996b. Frequency-dependent susceptibility measurements of environmental samples. Geophysical Journal International, 124: 228-240.

Dearing, J.A., Hannam, J.A., Landmine detection and soil magnetism: a global assessment. Submitted to Environmental Science and Technology.

Dearing, J.A., Hannam, J.A., Huddleston, A.S., Wellington, E.M.H., 2001a. Magnetic, geochemical and DNA properties of highly magnetic soils in England, Geophysical Journal International 144: 183-196.

Dearing, J.A., Hay, K., Baban, S., Huddleston, A.S., Wellington, E.M.H., Loveland, P.J., 1996a. Magnetic susceptibility of topsoils: a test of conflicting theories using a national database. Geophysical Journal International 127: 728-734.

Dearing, J.A., Lees, J.A., White, C., 1995. Mineral magnetic properties of gleyed soils under Oak and Corsican Pine. Geoderma 68: 309-319.

Dearing, J.A., Livingstone, I.P., Bateman, M.D., White, K.H., 2001b. Palaeoclimate records from OIS 8.0-5.4 recorded in loess-palaeosol sequences on the Matmata Plateau, southern Tunisia, based on mineral magnetism and new luminescence dating. Quaternary International 76/77: 43-56.

Dearing, J.A., Maher, B.A., Oldfield, F., 1985. Geomorphological linkages between soils and sediments: the role of magnetic measurements, In: K.S. Richards, R.R. Arnett, S. Ellis, (Editors), Geomorphology and Soils. Allen and Unwin, London, pp. 245-266.

de Jong, E., Kozak, L.M., Rostad, H.P.W., 1999. Effects of parent material and climate on the magnetic susceptibility of Saskatchewan soils. Canadian Journal of Soil Science 80: 135-142.

de Jong, E., Nestor P.A., Pennock D.J., 1998. The use of magnetic susceptibility to measure long-term soil redistribution. Catena 32: 23-35.

de Jong, E., Pennock D.J., Nestor P.A., 2000. Magnetic susceptibility of soils in different slope positions in Saskatchewan, Canada. Catena 40: 291-305.

Ďurža, O., 1999. Heavy metals contamination and magnetic susceptibility in soils around metallurgical plant. Physics and Chemistry of the Earth Part a-Solid Earth and Geodesy 24, 541-543.

Fassbinder, J.W.E., Stanjek, H.,Vali, H., 1990. Occurrence of magnetic bacteria in soil, Nature 343: 161-163.

Fialova, H., Maier, G., Petrovský, Kapička, A., Boyko, T., Scholger, R., 2006. Magnetic properties of soils from sites with different geological and environmental settings. Journal of Applied Geophysics 59: 273-283.

Flanders, P.J., 1994. Collection, measurement, and analysis of airborne magnetic particulates from pollution in the environment (invited). Journal of Applied Physics 75, 5931-5936.

Han, J., Lu, H., Wu, N., Guo, Z., 1996. Magnetic susceptibility of modern soils in China and climate conditions. Studia Geophysica et Geodetica 40: 262-275.

Hanesch, M., Petersen, N., 1999. Magnetic properties of a recent parabrown-earth from Southern Germany, Earth and Planetary Science Letters 169: 85-97.

Hanesch, M., Scholger, R., Dekkers, M.J., 2001 The application of fuzzy c-means cluster analysis and non-linear mapping to a soil data set for the detection of polluted sites. Phys Chem Earth 26: 885–891.

Hanesch, M., Rantitsch, G., Hemetsberger, S. Scholger, R., 2007. Lithological and pedological influences on the magnetic susceptibility of soil: Their consideration in magnetic pollution mapping. Science of the Total Environment 382, 351-363.

Hannam, J.A., 1999. Processes and timescales of secondary magnetic mineral formation in topsoils. Ph.D. Thesis, University of Liverpool, Liverpool.

Hannam, J.A., Dearing, J.A., 2008. Mapping soil magnetic properties in Bosnia and Herzegovina for landmine clearance operations, Earth and Planetary Science Letters 274, 285-294.

Hansel, C.M., Benner, S.G., Neiss, J., Dohnalkova, A., Kukkadapu, R.K., Fendorf, S., 2003. Secondary mineralization pathways induced by dissimilatory iron reduction of ferrihydrite under advective flow. Geochimica et Cosmochimicha Acta 67: 2977-2992.

Hay, K.L., Dearing, J.A., Baban, S.M.J., Loveland, P.J., 1997. A preliminary attempt to identify atmospherically-derived pollution particles in English topsoils from magnetic susceptibility measurements. Physics and Chemistry of the Earth 22: 207-210.

Heller, F., Liu, T.S., 1986. Palaeoclimatic and sedimentary history from magnetic susceptibility of loess in China. Geophysical Research Letters., 13: 1169-1172.

Hodgson, J.M., (Editor) 1976. Soil Survey Field Handbook. Soil Survey Technical Monograph No. 5, Harpenden.

Hounslow, M.W., Maher, B.A., 1996. Quantitative extraction and analysis of carriers of magnetization in sediments, Geophysical Journal International 124: 57 74.

Jenny, H., 1941. Factors of Soil Formation - A System of Quantitative Pedology. McGraw-Hill, New York. 109 pp.

Kapicka, A., Petrovsky, E., Ustjak, S., Machackova, K., 1999. Proxy mapping of fly-ash pollution of soils around a coal-burning power plant: a case study in the Czech Republic. Journal of Geochemical Exploration 66, 291-297.

Le Borgne E., 1955. Susceptibilité magnetique anormale du sol superficiel. Ann. Geophysique. 11: 399-419.

Le Borgne, E., 1960. Influence du feu sur les propriétés magnétique du sol et sur celles du schiste et du granit, Ann. Géophysique. 16: 159-195.

Liu, X., Rolph, T., Bloemendal, J., Shaw, J., Liu, T., 1995. Quantitative estimates of palaeoprecipitation at Xifeng, in the Loess Plateau of China. Palaeogeography Palaeoclimatology Palaeoecology 113: 243-248.

Liu,Q., Barrón, V., Torrent, J., Eeckhout, S.G., Deng, C., 2008. Magnetism of intermediate hydromaghemite in the transformation of 2-line ferrihydrite into hematite and its paleoenvironmental implications. Journal of Geophysical Research 113: B01103, doi:10.1029/2007JB005207.

Magiera, T., Strzyszcz, Z., 2000. Ferrimagnetic minerals of anthropogenic origin in soils of some Polish National Parks. Water, Air and Soil Pollution 124: 37-48.

Magiera, T., Stryszcz, Z., Kapička, A., Petrovský, E., 2006. Discrimination of lithogenic and anthropogenic influences on topsoil magnetic susceptibility in Central Europe. Geoderma 130: 299-311.

Maher, B.A., 1986. Characterisation of soils by mineral magnetic measurements. Physics of the Earth and Planetary Interiors 42: 76-92.

Maher, B.A., 1998. Magnetic properties of modern soils and Quaternary loessic paleosols: paleoclimatic implications. Paleogeography Paleoclimatology Paleoecology 137: 25-54.

Maher, B.A., Alekeev, A., Alekeev, T., 2002. Variation of soil magnetism across the Russia steppe: it’s significance for use of soil magnetism as a paleorainfall proxy. Quaternary Science Reviews 21: 1571-1576.

ACCEPTED MANUSCRIPT

Maher, B.A., Taylor, R.M., 1988. Formation of ultra fine-grained magnetite in soils, Nature 336: 368-370.

Maher, B.A., Thompson, R., 1995. Paleorainfall reconstructions from pedogenic magnetic susceptibility variations in the Chinese loess and paleosols. Quaternary Research 44: 383-391.

McGrath, S.P., Loveland, P.J., 1992. Soil Geochemical Atlas of England and Wales, Blackie, Glasgow.

Moukarika, A., O'Brien, F., Coey, J.M.D., 1991. Development of magnetic soil from ferroan dolomite. Geophys. Res. Lett. 18: 2043-2046.

Mullins, C.E., 1977. Magnetic susceptibility of the soil and its significance in soil science: a review. Journal of Soil Science 28: 223-246.

Neumeister, H., Peschel, G., 1968. Die magnetische Suszeptibilitat von Boden und pleistozanen Sedimentan in der Umgebung Leipzigs. Albrecht-Thaer-Archiv 12: 1055-1072.

Oldfield, F., Thompson, R., Barber, K.E., 1978. Changing atmospheric fallout of magnetic particles recorded in recent ombrotrophic peat sections. Science 199: 679-80.

Oldfield, F., Crowther, J., 2007. Establishing fire incidence in temperate soils using magnetic measurements. Palaeogeography, Palaeoclimatology, Palaeoecology 249:

362-369.

Perry, M., Hollis, D., 2004. The generation of monthly gridded datasets for a range of climatic variables over the UK. International Journal of Climatology 25: 1041-1054.

Rasmussen, P.E., Rickman, R.W., Douglas, J.C.L., Air and soil temperatures during Spring burning of standing wheat stubble. Agronomy Journal 78, 261-263.

Retallack, G.J., Sheldon, N.D., Cogoini, M., Elmore, R.D., 2003. Magnetic susceptibility of early Paleozoic and Precambrian paleosols. Palaeogeography, Palaeoclimatology, Palaeoecology 198: 373-380.

Rummery, T.A., Bloemendal, J., Dearing, J.A., Oldfield, F., Thompson, R., 1979. The persistence of fire-induced magnetic oxides in soil and lake sediments. Annales de Géophysique 35: 103–107.

Schwertmann, U., 1988. Occurrence and formation of iron oxides in various pedoenvironments. In: J.W. Stuki, B.A. Goodman, U. Schwertmann (Editors), Iron Oxides in Soils and Clay Minerals. Reidel Publishing Co.

Schwertmann, U., Taylor R.M., 1989. Iron Oxides. In: J.B. Dixon, S.B. Weed (Editors), Minerals in Soil Environments SSSA Book Series No. 1, Soil Science Society of America.

Singer, M.J., Fine, P., 1989. Peodgenic factors affecting magnetic susceptibility of northern California soils. Soil Science Society of America Journal 53: 1119-1127.

Singer, M.J., Fine, P., Verosub, K.L., Chadwick, O.A., 1992. Time dependence of magnetic susceptibility of soil chronosequences on the California coast. Quaternary Research 37: 322-332.

Singer, M.J., Verosub, K.L., Fine, P., TenPas, J., 1996. A conceptual model for the enhancement of magnetic susceptibility in soils. Quaternary International Journal 34-36: 2443-2458.

Stanjek, H., Fassbinder, J.W.E., Vali, H., Wagele, H., Graf, W., 1994. Evidence of biogenic greigite (ferrimagnetic Fe3S4) in soil. European Journal of Soil Science 45: 97-104.

Tite, M. S., 1972. The influence of geology on the magnetic susceptibility of soils on archaeological Sites. Archaeometry 14: 229-236.

Tite, M. S., Mullins, C.E., 1970. Electromagnetic Prospecting on Archaeological Sites Using a Soil Conductivity Meter. Archaeometry 12: 97-104.

Thompson, R., Oldfield, F., 1986. Environmental magnetism. Allen and Unwin, London, UK. pp. 227.

Thompson, R., Bloemendal, J., Dearing, J.A., Oldfield, F., Rummery, T.A., Stober, J.C., 1980. Environmental applications of magnetic measurements. Science 207, 481-486.

Thompson, R., Battarbee, R.W., O'Sullivan, P.E., Oldfield, F., 1975. Magnetic susceptibility of lake sediments. Limnology and Oceanography 20: 687-698.

Torrent, J., Schwertmann, U., and Schulze, D. G., 1980. Iron oxide mineralogy of some soils of two river terrace sequences in Spain. Geoderma 23: 191-208.

Torrent, J., Barrón, V., Liu, Q., 2006. Magnetic enhancement is linked to and precedes hematite formation in aerobic soil. Geophysical Research Letters 33: L0240I, doi:10.1029/2005GL024818.

Vali, H., Dobenck, T. von, Amarantidis, G., Forster, O., Mortenani, G., Bachmann, L., Petersen, N., 1989. Biogeneic and lithogenic magnetic minerals. In: Atlantic and Pacific deep-sea sediments and their palaeomagnetic significance. Geologische Rundschau 78: 753–764.

Vidic, N.J., Singer, M.J., Verosub, K.L., 2004. Duration dependence of magnetic susceptibility enhancement in the Chinese loess–palaeosols of the past 620 ky. Palaeogeography, Palaeoclimatology, Palaeoecology 211: 271-288.

Walden, J., Oldfield, F., Smith, J.P., (eds) 1999. Environmental Magnetism: a practical guide. Technical guide, No. 6. Quaternary Research Association, London.

Walling, D.E., Peart, M.R., Oldfield, F., Thompson, R., 1979. Suspended sediments sources identified by magnetic measurements, Nature 281: 110-113.

Figure 1

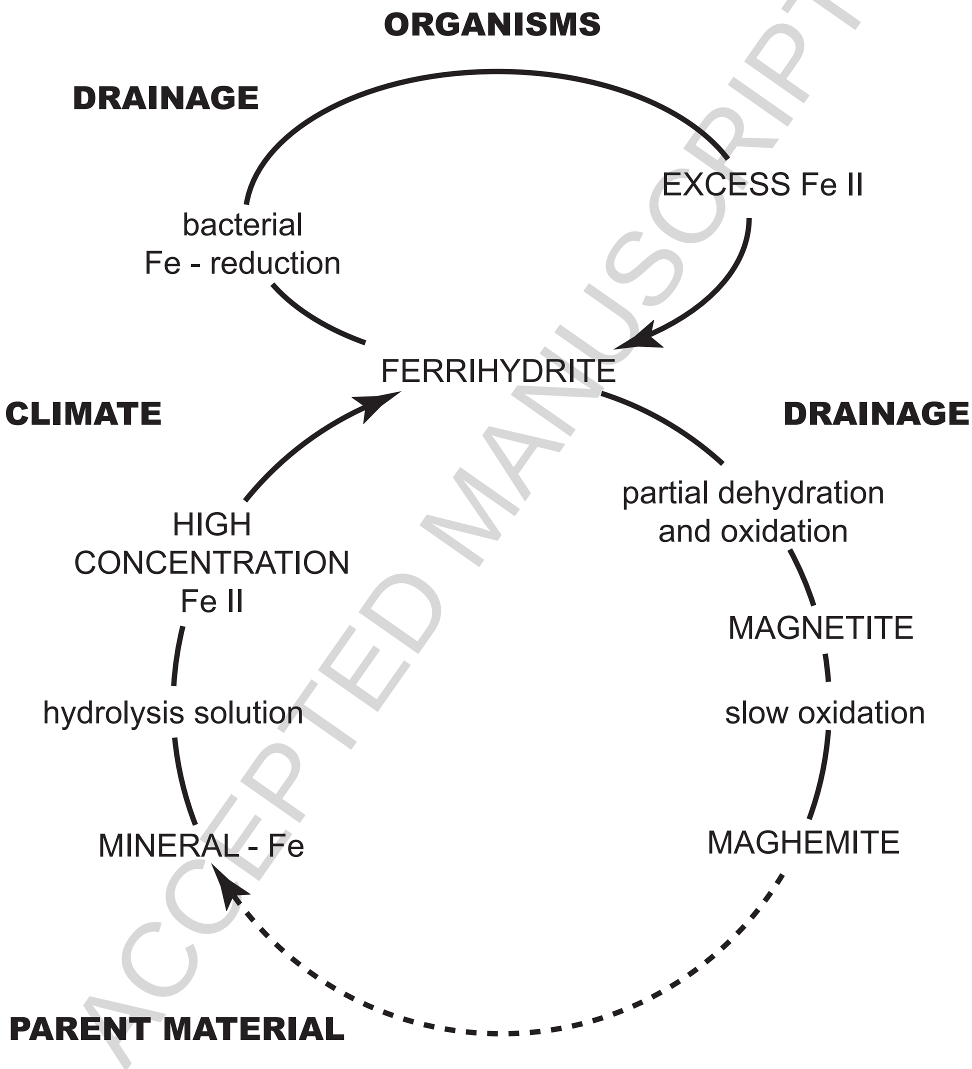
ORGANISMS
DRAINAGE
EXCESS Fe II
bacterial
Fe - reduction
FERRIHYDRITE
CLIMATE
DRAINAGE
partial dehydration
and oxidation
HIGH
CONCENTRATION
Fe II
MAGNETITE
hydrolysis solution
slow oxidation
MINERAL - Fe
MAGHEMITE
PARENT MATERIAL

Figure 2

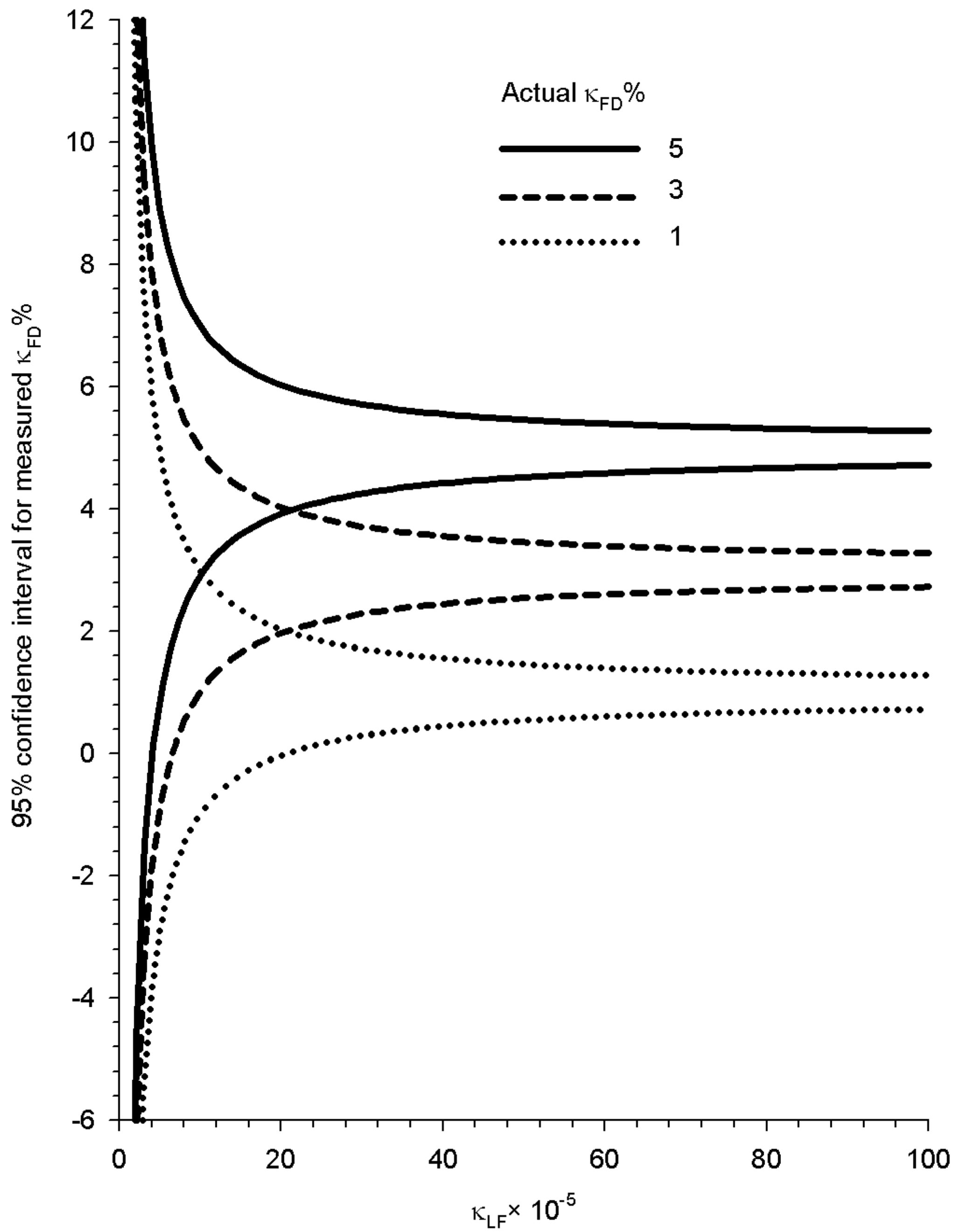
Actual κFD%
5
3
1
95% confidence interval for measured κFD%
κLF× 10-5
12
10
8
6
4
2
0
-2
-4
-6
0
20
40
60
80
100

Figure 3

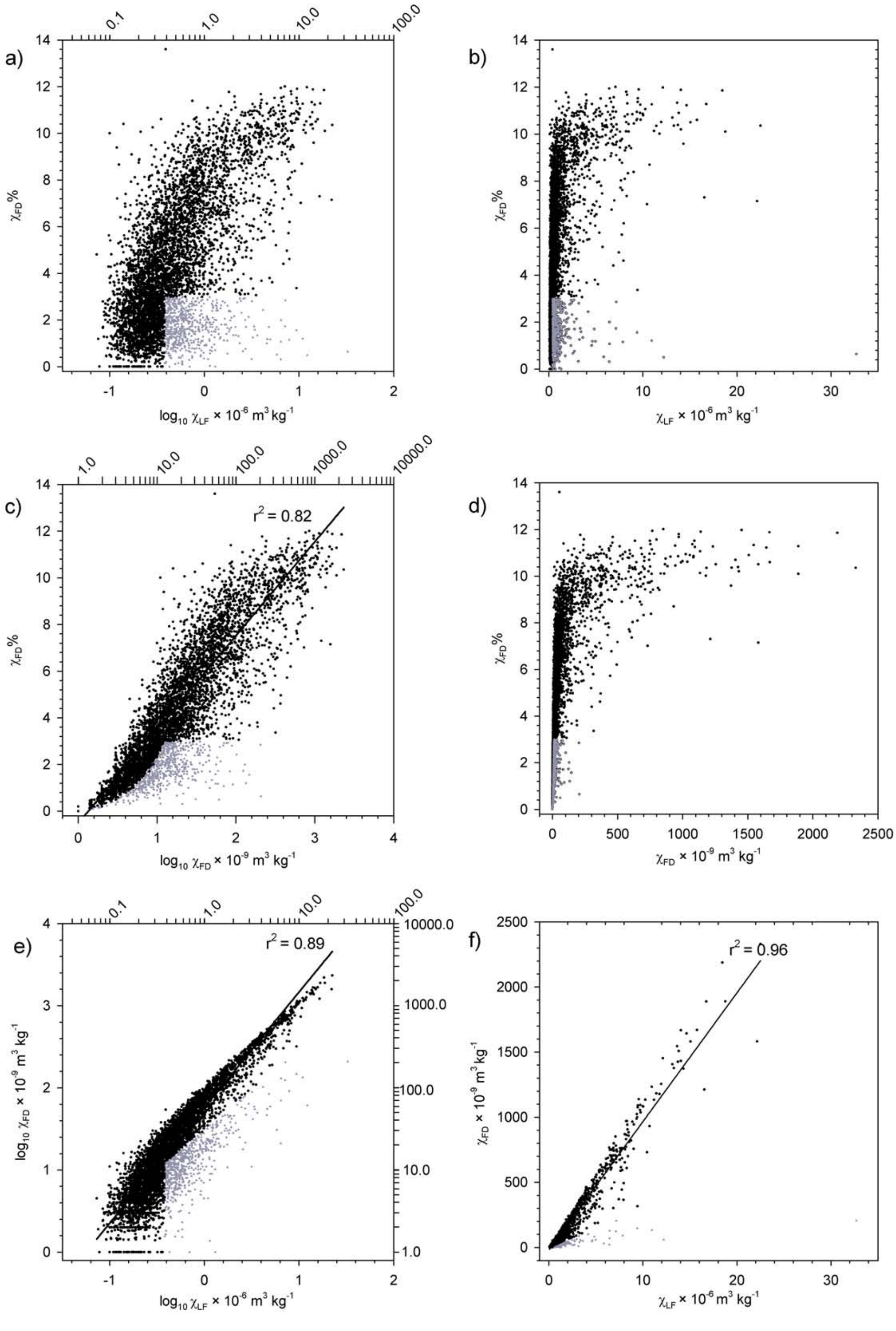
a)
b)
c)
d)
e)
f)
χ_{FD}%
$\log_{10} \chi_{LF} \times 10^{-6}$ m^3 kg^{-1}
$\chi_{LF} \times 10^{-6}$ m^3 kg^{-1}
$\log_{10} \chi_{FD} \times 10^{-9}$ m^3 kg^{-1}
$\chi_{FD} \times 10^{-9}$ m^3 kg^{-1}
r^2 = 0.82
r^2 = 0.89
r^2 = 0.96

Figure 4

a) b) $\chi_{LF} \times 10^{-6}$ m^3 kg^{-1}

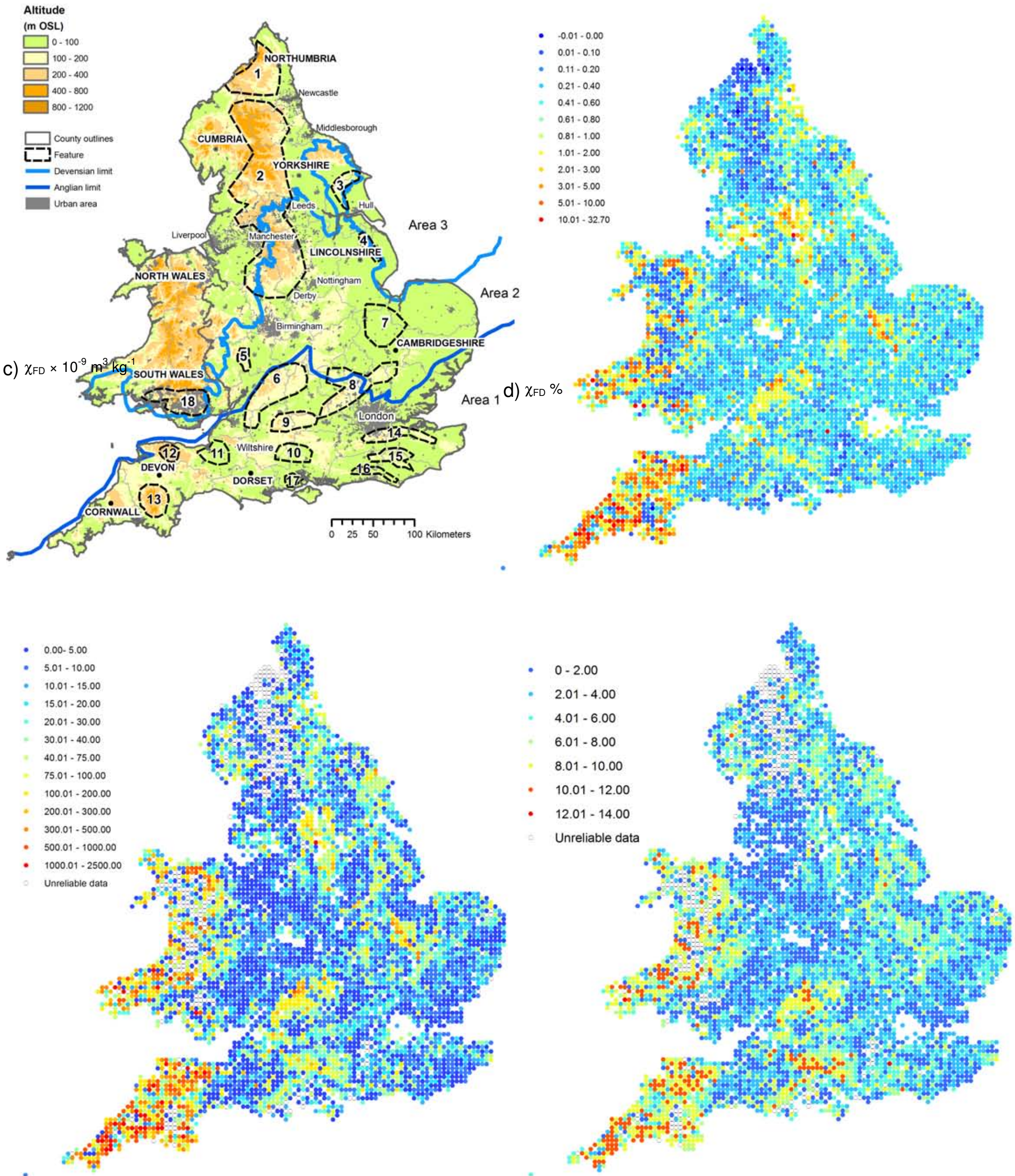

Figure 5

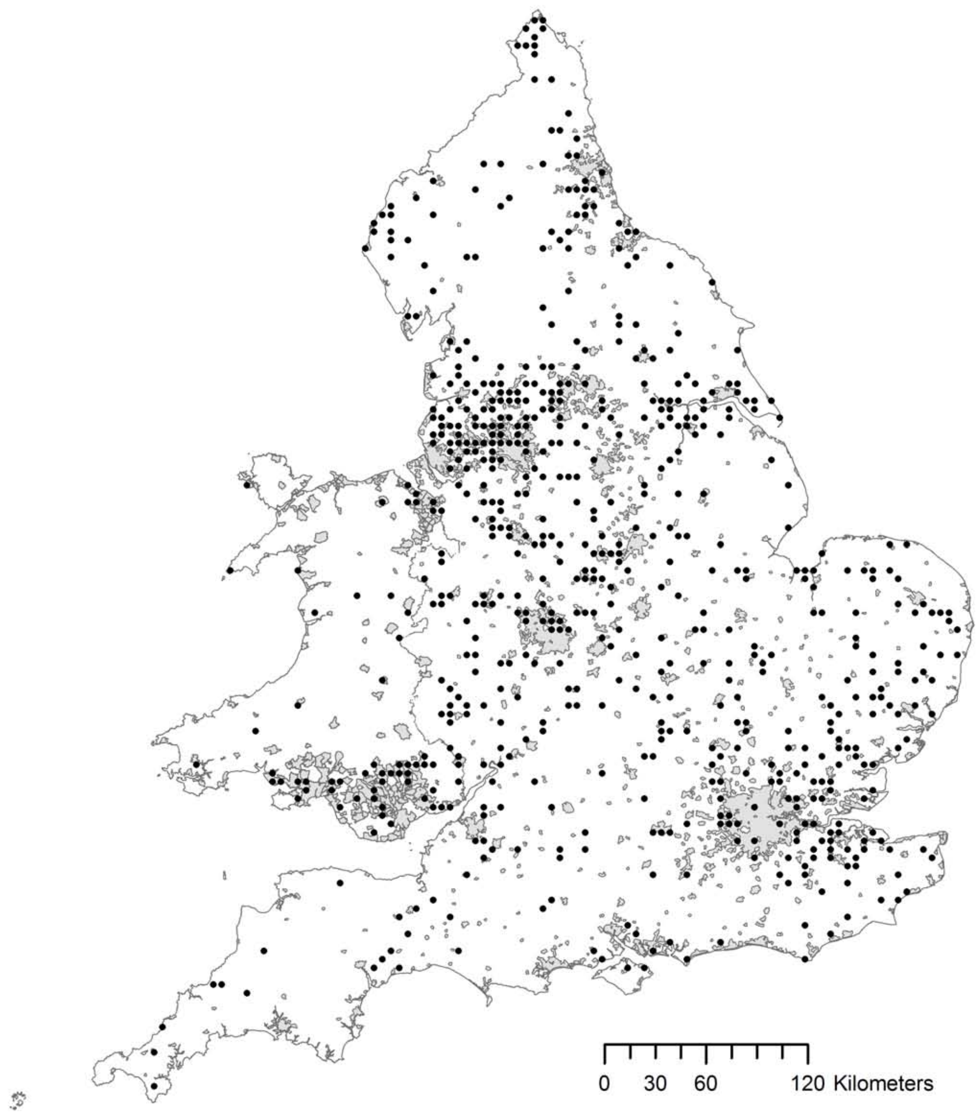

Figure 6

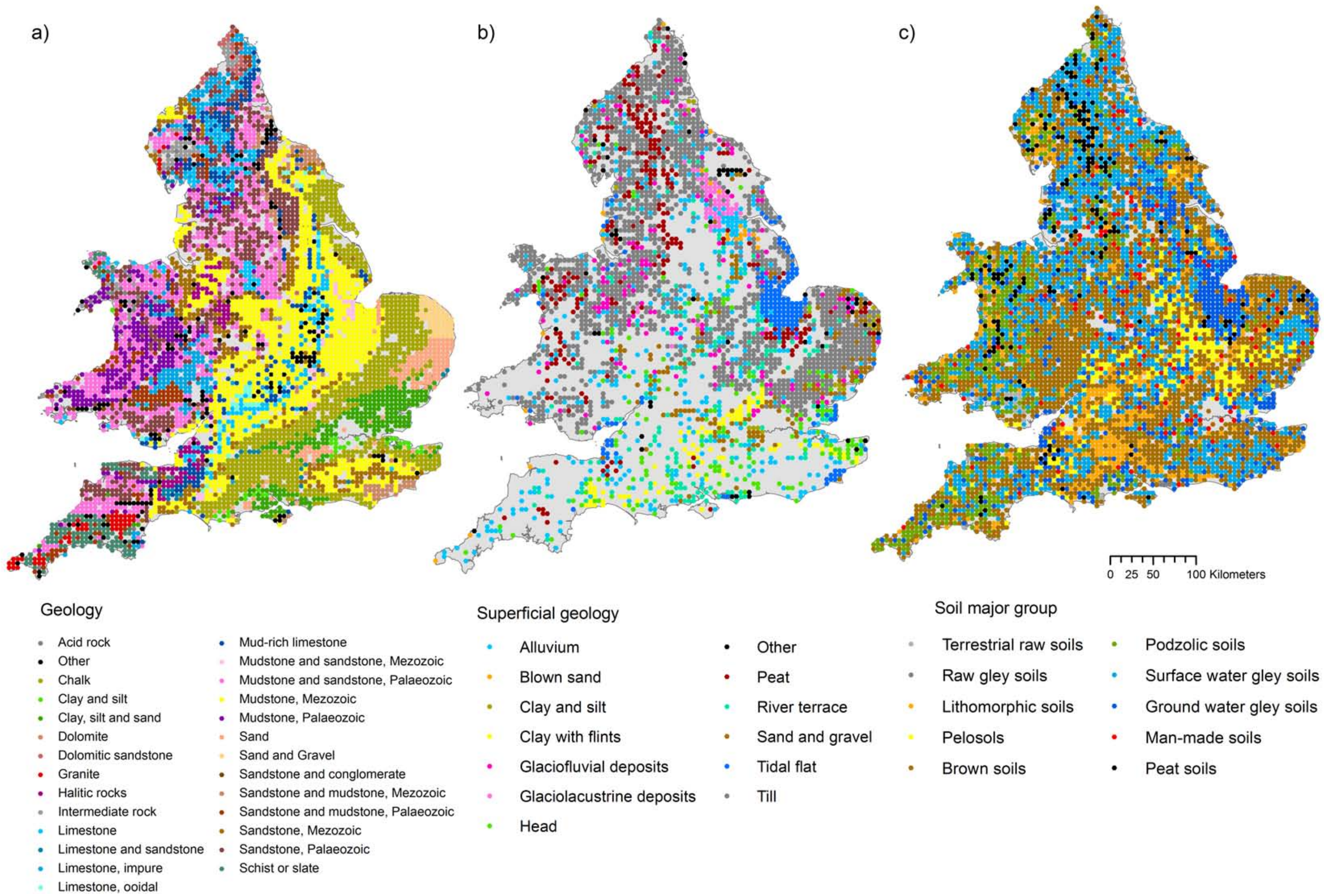
a)
b)
c)
0 25 50 100 Kilometers
Geology
Acid rock
Other
Chalk
Clay and silt
Clay, silt and sand
Dolomite
Dolomitic sandstone
Granite
Halitic rocks
Intermediate rock
Limestone
Limestone and sandstone
Limestone, impure
Limestone, ooidal
Mud-rich limestone
Mudstone and sandstone, Mezozoic
Mudstone and sandstone, Palaeozoic
Mudstone, Mezozoic
Mudstone, Palaeozoic
Sand
Sand and Gravel
Sandstone and conglomerate
Sandstone and mudstone, Mezozoic
Sandstone and mudstone, Palaeozoic
Sandstone, Mezozoic
Sandstone, Palaeozoic
Schist or slate
Superficial geology
Alluvium
Blown sand
Clay and silt
Clay with flints
Glaciofluvial deposits
Glaciolacustrine deposits
Head
Other
Peat
River terrace
Sand and gravel
Tidal flat
Till
Soil major group
Terrestrial raw soils
Raw gley soils
Lithomorphic soils
Pelosols
Brown soils
Podzolic soils
Surface water gley soils
Ground water gley soils
Man-made soils
Peat soils

Figure 7

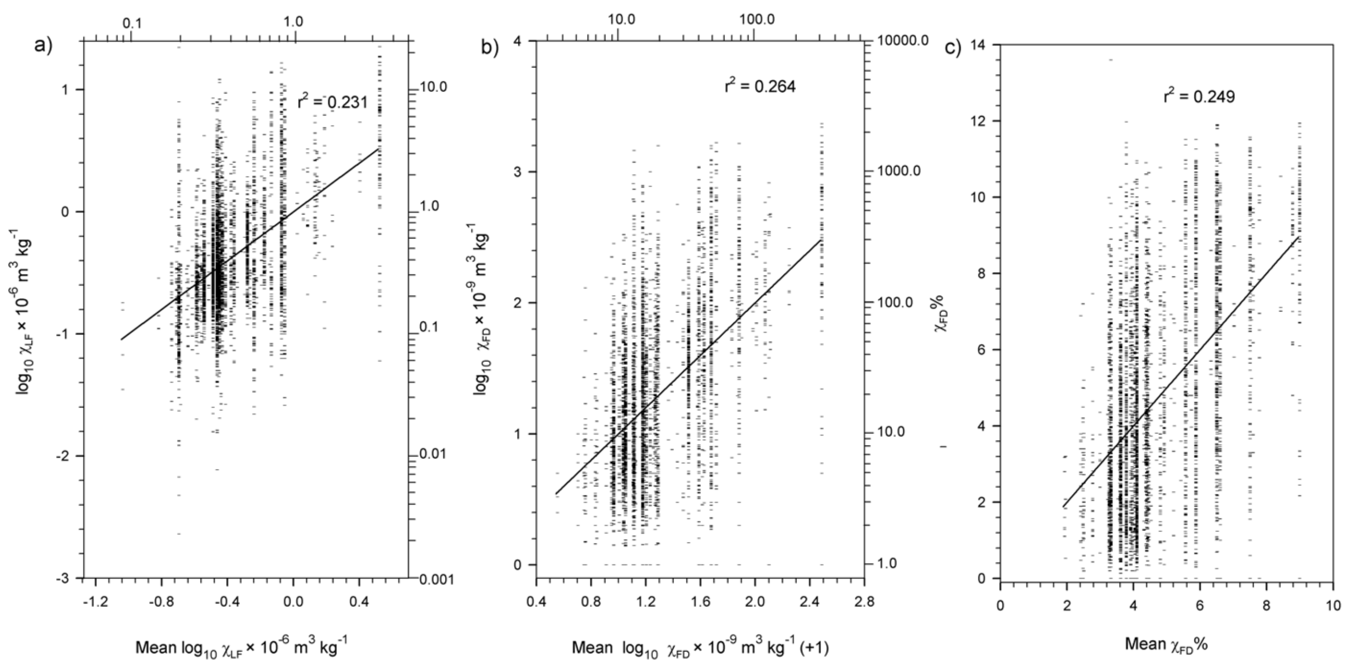
a)
r² = 0.231
0.1
1.0
10.0
0.01
0.001
log10 χLF × 10-6 m3 kg-1
Mean log10 χLF × 10-6 m3 kg-1
b)
r² = 0.264
10.0
100.0
10000.0
1000.0
1.0
log10 χFD × 10-9 m3 kg-1
Mean log10 χFD × 10-9 m3 kg-1 (+1)
c)
r² = 0.249
χFD%
Mean χFD%

Figure 8

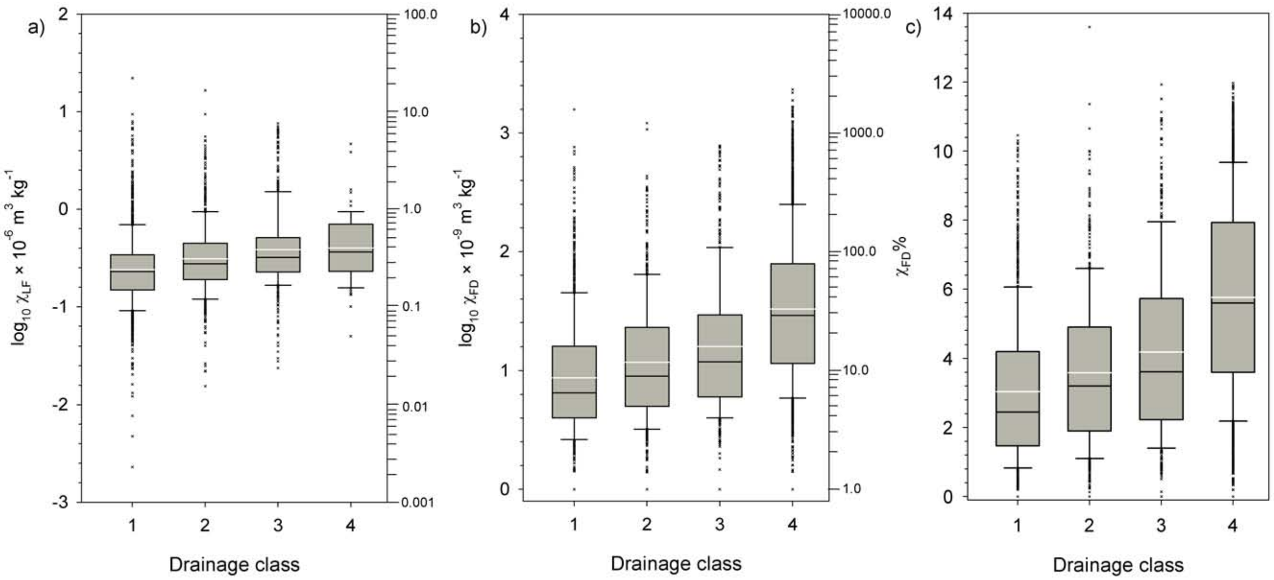
a)
b)
c)
Drainage class
Drainage class
Drainage class
1
2
3
4
100.0
10.0
1.0
0.1
0.01
0.001
10000.0
1000.0
100.0
10.0
1.0
14
12
10
8
6
4
2
0

Figure 9

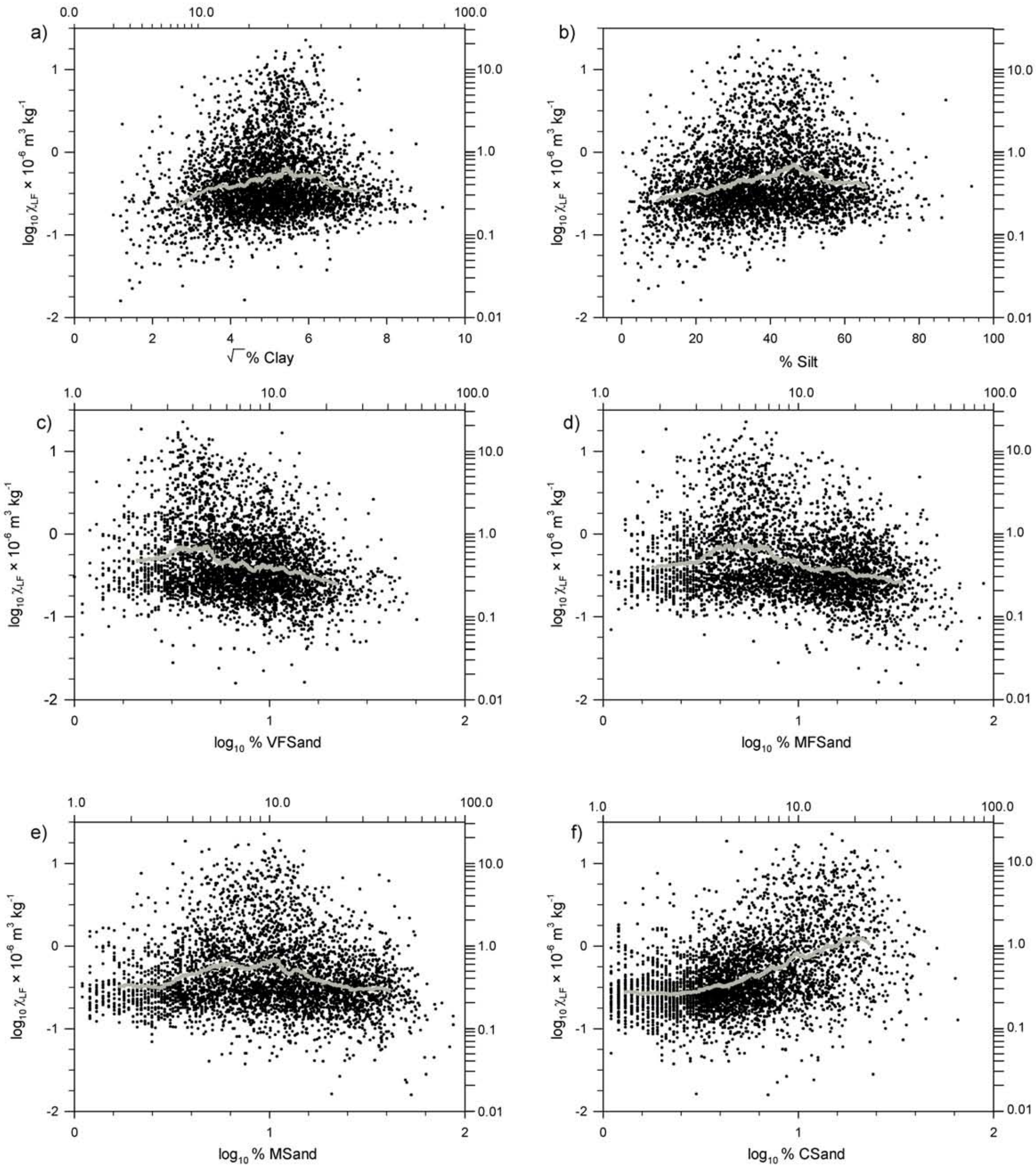
a)
b)
c)
d)
e)
f)
log10 χLF × 10-6 m3 kg-1
√ % Clay
% Silt
log10 % VFSand
log10 % MFSand
log10 % MSand
log10 % CSand

Figure 10

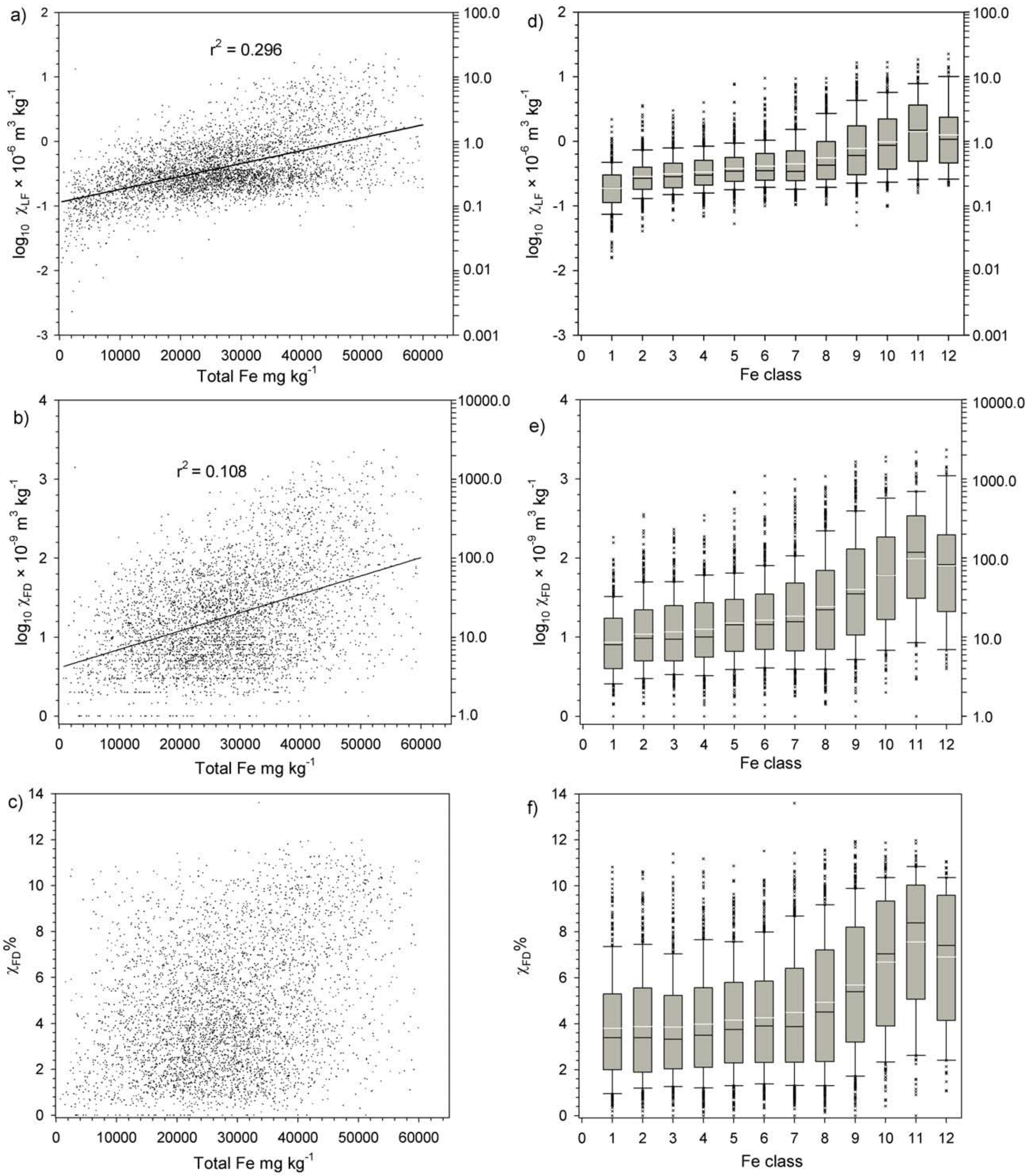

a)
r² = 0.296
log10 χLF × 10-6 m3 kg-1
Total Fe mg kg-1
b)
r² = 0.108
log10 χFD × 10-9 m3 kg-1
Total Fe mg kg-1
c)
χFD%
Total Fe mg kg-1
d)
log10 χLF × 10-6 m3 kg-1
Fe class
e)
log10 χFD × 10-9 m3 kg-1
Fe class
f)
χFD%
Fe class

Figure 11

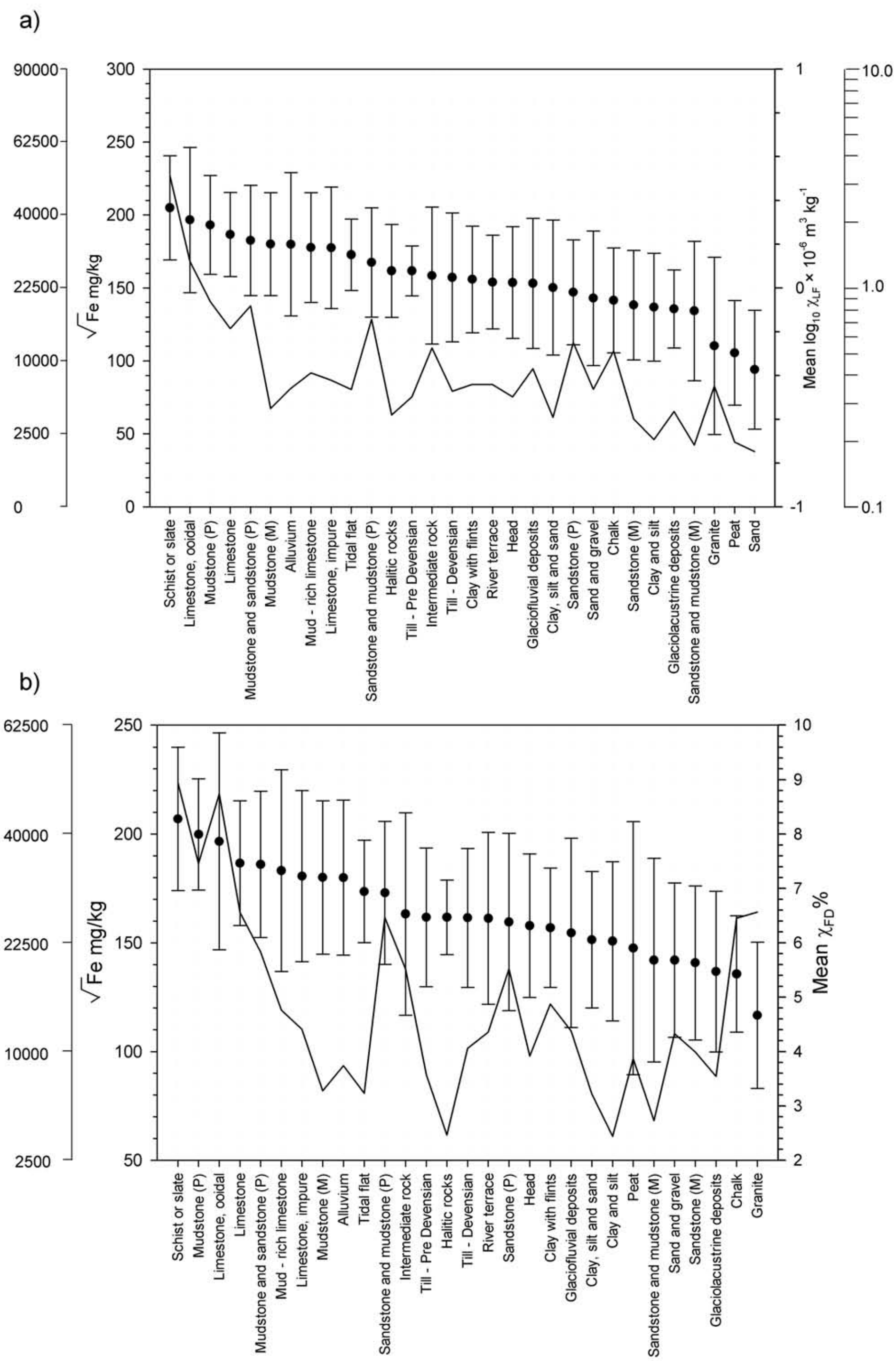
a)
90000
62500
40000
22500
10000
2500
0
300
250
200
150
100
50
0
√Fe mg/kg
1
-1
Mean log₁₀ χLF × 10⁻⁶ m³ kg⁻¹
10.0
1.0
0.1
Schist or slate
Limestone, ooidal
Mudstone (P)
Limestone
Mudstone and sandstone (P)
Mudstone (M)
Alluvium
Mud - rich limestone
Limestone, impure
Tidal flat
Sandstone and mudstone (P)
Halitic rocks
Till - Pre Devensian
Intermediate rock
Till - Devensian
Clay with flints
River terrace
Head
Glaciofluvial deposits
Clay, silt and sand
Sandstone (P)
Sand and gravel
Chalk
Sandstone (M)
Clay and silt
Glaciolacustrine deposits
Sandstone and mudstone (M)
Granite
Peat
Sand
b)
62500
40000
22500
10000
2500
250
200
150
100
50
√Fe mg/kg
10
9
8
7
6
5
4
3
2
Mean χFD %
Schist or slate
Mudstone (P)
Limestone, ooidal
Limestone
Mudstone and sandstone (P)
Mud - rich limestone
Limestone, impure
Mudstone (M)
Alluvium
Tidal flat
Sandstone and mudstone (P)
Intermediate rock
Till - Pre Devensian
Halitic rocks
Till - Devensian
River terrace
Sandstone (P)
Head
Clay with flints
Glaciofluvial deposits
Clay, silt and sand
Clay and silt
Peat
Sandstone and mudstone (M)
Sand and gravel
Sandstone (M)
Glaciolacustrine deposits
Chalk
Granite

Figure 12

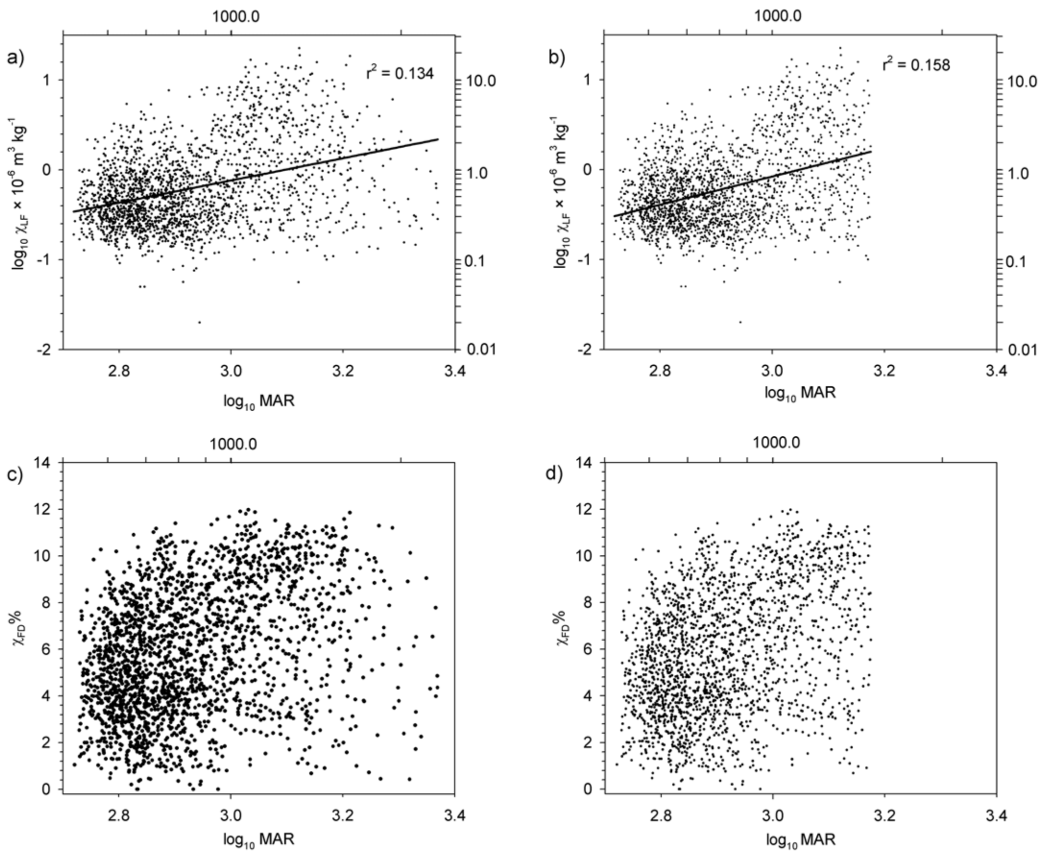
a)
b)
c)
d)
1000.0
r² = 0.134
r² = 0.158
log10 χLF × 10-6 m3 kg-1
χFD%
log10 MAR
10.0
1.0
0.1
0.01
2.8
3.0
3.2
3.4

Figure 13

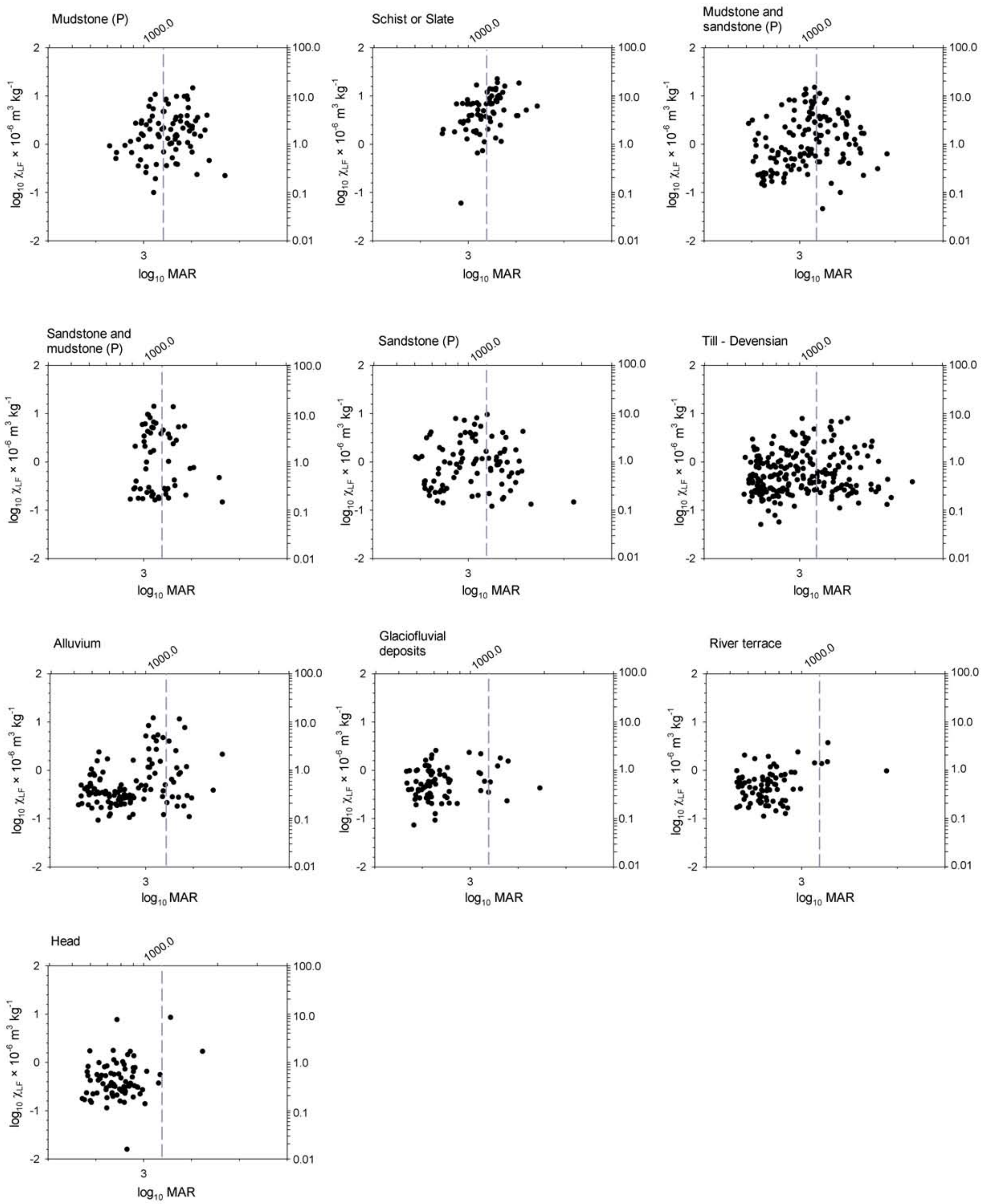

Mudstone (P)
Schist or Slate
Mudstone and sandstone (P)
Sandstone and mudstone (P)
Sandstone (P)
Till - Devensian
Alluvium
Glaciofluvial deposits
River terrace
Head
1000.0
100.0
10.0
1.0
0.1
0.01
2
1
0
-1
-2
3
log10 MAR
log10 χLF × 10-6 m3 kg-1

Figure 14

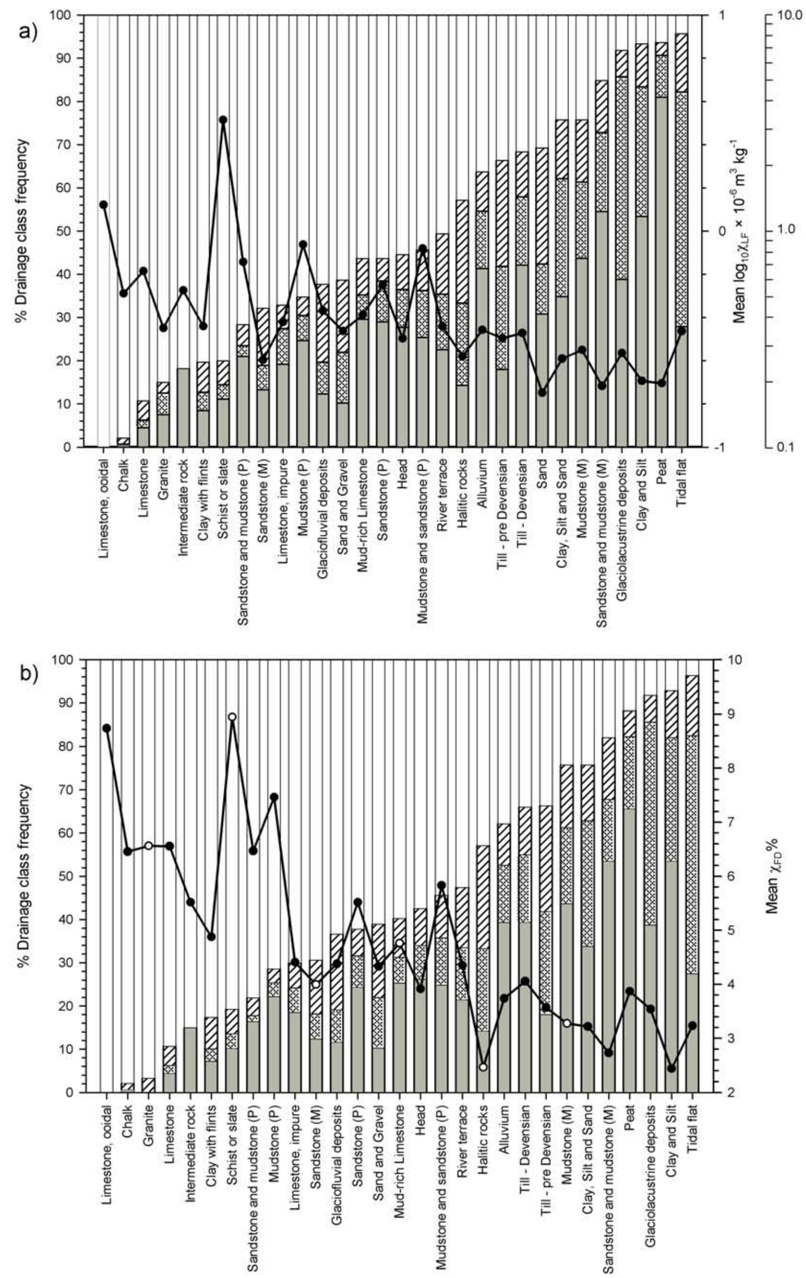
a)
% Drainage class frequency
Mean $\log_{10}\chi_{LF} \times 10^{-6}$ m^3 kg^{-1}
Limestone, ooidal
Chalk
Limestone
Granite
Intermediate rock
Clay with flints
Schist or slate
Sandstone and mudstone (P)
Sandstone (M)
Limestone, impure
Mudstone (P)
Glaciofluvial deposits
Sand and Gravel
Mud-rich Limestone
Sandstone (P)
Head
Mudstone and sandstone (P)
River terrace
Halitic rocks
Alluvium
Till - pre Devensian
Till - Devensian
Sand
Clay, Silt and Sand
Mudstone (M)
Sandstone and mudstone (M)
Glaciolacustrine deposits
Clay and Silt
Peat
Tidal flat
b)
% Drainage class frequency
Mean χ_{FD}%
Limestone, ooidal
Chalk
Granite
Limestone
Intermediate rock
Clay with flints
Schist or slate
Sandstone and mudstone (P)
Mudstone (P)
Limestone, impure
Sandstone (M)
Glaciofluvial deposits
Sandstone (P)
Sand and Gravel
Mud-rich Limestone
Head
Mudstone and sandstone (P)
River terrace
Halitic rocks
Alluvium
Till - Devensian
Till - pre Devensian
Mudstone (M)
Clay, Silt and Sand
Sandstone and mudstone (M)
Peat
Glaciolacustrine deposits
Clay and Silt
Tidal flat

Figure 15

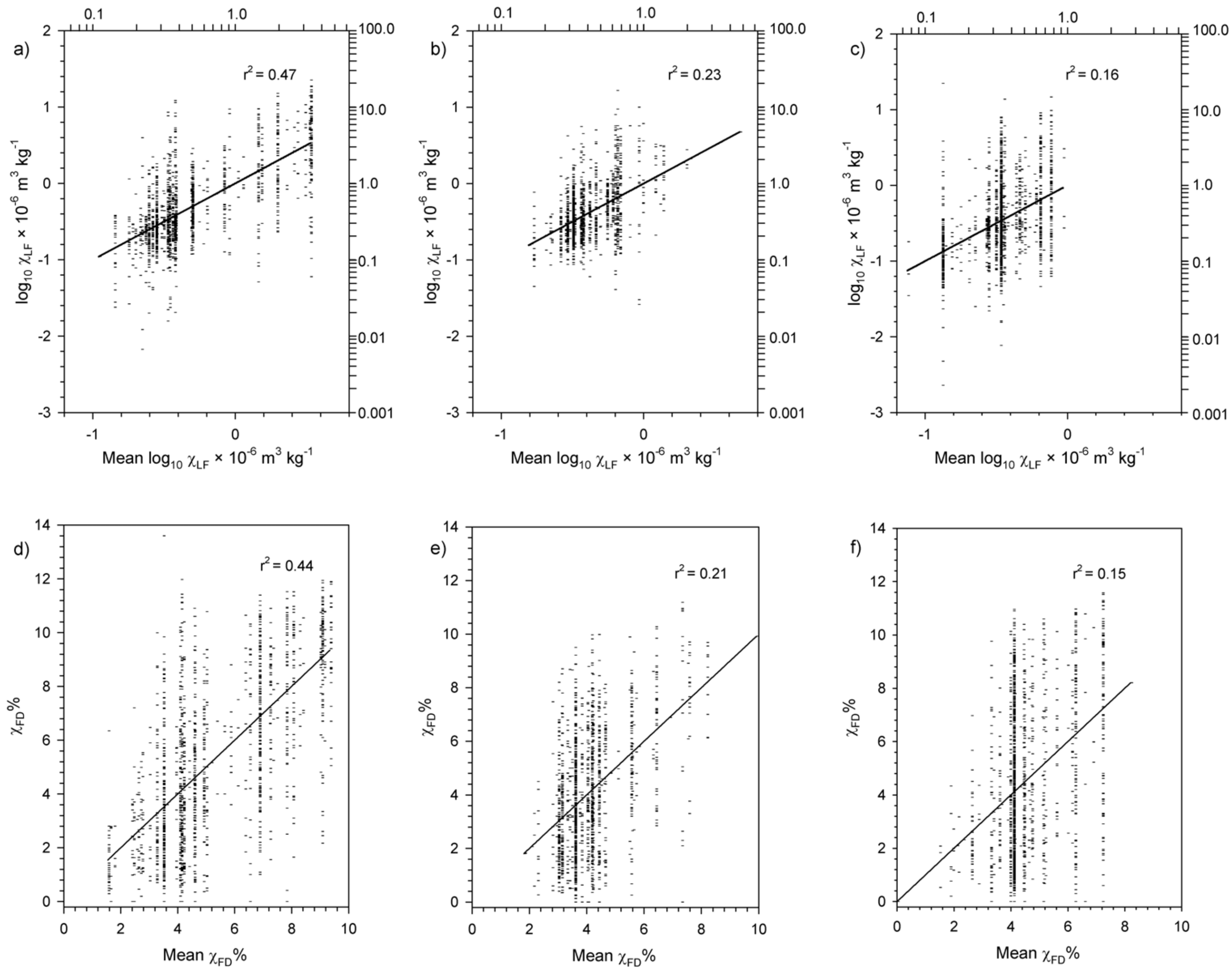
a)
b)
c)
d)
e)
f)
r² = 0.47
r² = 0.23
r² = 0.16
r² = 0.44
r² = 0.21
r² = 0.15
log10 χLF × 10-6 m3 kg-1
Mean log10 χLF × 10-6 m3 kg-1
χFD%
Mean χFD%

Figure 16

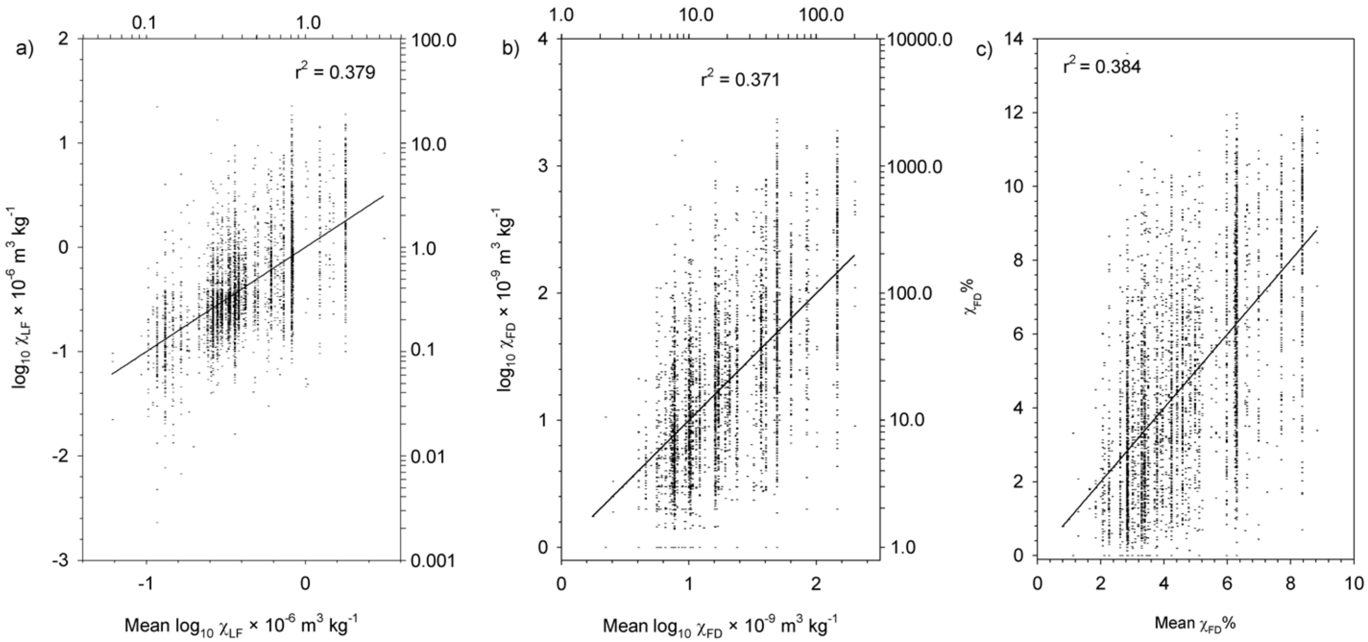
a)
r² = 0.379
log10 χLF × 10-6 m3 kg-1
Mean log10 χLF × 10-6 m3 kg-1
b)
r² = 0.371
log10 χFD × 10-9 m3 kg-1
Mean log10 χFD × 10-9 m3 kg-1
c)
r² = 0.384
χFD%
Mean χFD%

Table 1

Statistics	All magnetic samples			Reduced dataset		
	$\chi_{LF} \times 10^{-6}$ m^3 kg^{-1}	$\chi_{FD} \times 10^{-9}$ m^3 kg^{-1}	χ_{FD}%	$\chi_{LF} \times 10^{-6}$ m^3 kg^{-1}	$\chi_{FD} \times 10^{-9}$ m^3 kg^{-1}	χ_{FD}%
n	5656	5279	5279	4896	4535	4535
Mean	0.83	58.54	4.26	0.81	64.39	4.60
Geometric Mean	0.42	16.88	3.55	0.40	17.81	3.88
Median	0.37	13.33	3.60	0.32	14.37	4.07
Range	32.71	2329.32	13.60	22.50	2329.32	13.60
Minimum	-0.01	0.00	0.00	0.00	0.00	0.00
Maximum	32.70	2329.32	13.60	22.50	2329.32	13.60
Standard deviation	1.61	156.60	2.77	1.60	166.43	2.78
Sample variance	2.58	24522.07	7.70	2.55	27699.91	7.72
Coefficient of variation	194.20	267.52	65.08	196.82	258.46	60.43
Kurtosis	64.43	51.23	-0.48	42.60	45.44	-0.65
Skewness	6.39	6.22	0.68	5.57	5.87	0.52
Percentiles						
10	0.14	2.88	1.18	0.13	2.62	1.30
20	0.20	4.67	1.75	0.19	4.26	2.00
30	0.25	6.70	2.30	0.23	6.30	2.69
40	0.30	9.09	2.90	0.27	9.00	3.38
50	0.37	13.33	3.60	0.32	14.37	4.07
60	0.46	19.50	4.42	0.40	22.27	4.93
70	0.61	30.00	5.54	0.57	35.45	6.00
80	0.87	53.06	6.89	0.84	61.87	7.20
90	1.64	118.88	8.59	1.67	137.09	8.83
95	3.19	276.00	9.70	3.30	310.15	9.84
98	6.29	593.26	10.44	6.43	637.39	10.56

Table 2

Parent material top 10	Count	Geometric Mean $\chi_{LF} \times 10^{-6}$ m^3 kg^{-1}	Parent material top 10	Count	Geometric Mean $\chi_{FD} \times 10^{-9}$ m^3 kg^{-1}	Parent material top 10	Count	Mean χ_{FD}%
Schist or Slate	90	3.26	Schist or Slate	88	300.08	Schist or Slate	88	8.95
Limestone, ooidal	32	1.32	Limestone, ooidal	32	115.32	Limestone, ooidal	32	8.74
Mudstone (P)	138	0.87	Mudstone (P)	126	74.59	Mudstone (P)	126	7.46
Mudstone and sandstone (P)	276	0.83	Sandstone and mudstone (P)	73	50.12	Granite	30	6.56
Sandstone and mudstone (P)	81	0.72	Mudstone and sandstone (P)	265	46.36	Limestone	112	6.55
Limestone	112	0.64	Limestone	112	41.35	Sandstone and mudstone (P)	73	6.47
Sandstone (P)	190	0.56	Granite	30	40.02	Chalk	281	6.45
Intermediate rock	22	0.54	Sandstone (P)	164	37.71	Mudstone and sandstone (P)	265	5.83
Chalk	281	0.51	Chalk	281	31.84	Sandstone (P)	164	5.52
Glaciofluvial deposits	122	0.42	Intermediate rock	20	29.01	Intermediate rock	20	5.52
Parent material bottom 10			Parent material bottom 10			Parent material bottom 10		
Head	148	0.32	Head	141	12.51	Peat	102	3.87
Mudstone (M)	318	0.28	Till - pre Devensian	437	11.00	Alluvium	325	3.74
Glaciolacustrine deposits	49	0.27	Tidal flat	138	10.66	Till - pre Devensian	437	3.57
Halitic rocks	21	0.26	Sandstone (M)	137	10.57	Glaciolacustrine deposits	49	3.54
Clay, silt and sand	66	0.26	Glaciolacustrine deposits	49	9.89	Mudstone (M)	318	3.28
Sandstone (M)	143	0.25	Mudstone (M)	318	9.01	Tidal flat	138	3.23
Clay and silt	30	0.20	Clay, silt and sand	62	8.71	Clay, silt and sand	62	3.22
Peat	236	0.20	Halitic rocks	21	6.77	Sandstone and mudstone (M)	28	2.73
Sandstone and mudstone (M)	33	0.19	Sandstone and mudstone (M)	28	6.61	Halitic rocks	21	2.46
Sand	26	0.18	Clay and silt	28	5.59	Clay and silt	28	2.44

Table 3

Mean Annual Rainfall (mm)						Mean Annual Temperature (°C)					
Category	Lower boundary	Upper boundary	Geometric Mean $\chi_{LF} \times 10^{-6}$ m^3 kg^{-1}	Geometric Mean $\chi_{FD} \times 10^{-9}$ m^3 kg^{-1}	Mean χ_{FD}%	Category	Lower boundary	Upper boundary	Geometric Mean $\chi_{LF} \times 10^{-6}$ m^3 kg^{-1}	Geometric Mean $\chi_{FD} \times 10^{-9}$ m^3 kg^{-1}	Mean χ_{FD}%
1	≥ 507.27	< 591.91	0.38	13.17	3.88	1	≥ 4.18	< 7.57	0.19	11.55	4.03
2	≥ 591.91	< 623.52	0.35	12.53	3.90	2	≥ 7.57	< 8.31	0.39	19.69	4.84
3	≥ 623.52	< 661.815	0.37	13.33	3.91	3	≥ 8.31	< 8.76	0.49	22.64	4.94
4	≥ 661. 81	< 704.91	0.36	12.69	3.93	4	≥ 8.76	< 9.00	0.42	17.26	4.51
5	≥ 704.91	< 765.56	0.36	13.07	4.16	5	≥ 9.00	< 9.17	0.41	16.58	4.51
6	≥ 765.56	< 835.17	0.35	14.61	4.56	6	≥ 9.17	< 9.32	0.45	18.27	4.59
7	≥ 835.17	< 947.00	0.34	15.37	4.62	7	≥ 9.32	< 9.47	0.40	14.81	4.25
8	≥ 947.00	< 1109.04	0.64	40.46	6.10	8	≥ 9.47	< 9.64	0.42	17.33	4.65
9	≥ 1109.04	< 1382.43	0.63	45.28	6.10	9	≥ 9.64	< 9.89	0.42	17.36	4.56
10	≥ 1382.43	< 1633.60	0.48	39.95	6.07	10	≥ 9.89	< 10.13	0.38	14.83	4.26
11	≥ 1633.60	< 1970.109	0.24	19.61	4.83	11	≥ 10.13	< 10.38	0.57	23.76	4.96
12	≥ 1970.109	≤ 4134.38	0.19	12.40	3.82	12	≥ 10.38	≤ 11.54	1.00	59.05	6.46

Table 4

a)

Altitude class	Altitude (m) Lower boundary	Upper boundary	Geometric Mean $\chi_{LF} \times 10^{-6}$ m^3 kg^{-1}	Geometric Mean $\chi_{FD} \times 10^{-9}$ m^3 kg^{-1}	Mean χ_{FD}%
1	≥ -1	< 12	0.36	11.83	3.65
2	≥ 12	< 35	0.35	12.74	4.02
3	≥ 35	< 55	0.38	14.15	4.20
4	≥ 55	< 75	0.42	16.87	4.46
5	≥ 75	< 94	0.41	15.45	4.33
6	≥ 94	< 119	0.45	18.82	4.79
7	≥ 119	< 152	0.52	25.06	5.23
8	≥ 152	< 206	0.54	27.91	5.40
9	≥ 206	< 310	0.45	26.56	5.41
10	≥ 310	< 405	0.28	19.50	4.93
11	≥ 405	< 510	0.16	9.05	3.72
12	≥ 510	≤ 1400	0.21	15.45	4.12

b)

Slope class	Slope (°) Lower boundary	Upper boundary	Count	Geometric Mean $\chi_{LF} \times 10^{-6}$ m^3 kg^{-1}	Count	Geometric Mean $\chi_{FD} \times 10^{-9}$ m^3 kg^{-1}	Mean χ_{FD}%
1	≥ 0	< 2	1993	0.35	1908	12.92	3.97
2	≥ 2	< 5	1582	0.39	1446	17.19	4.54
3	≥ 5	< 10	821	0.49	731	28.82	5.46
4	≥ 10	< 15	235	0.49	201	33.04	5.78
5	≥ 15	< 20	122	0.56	110	36.75	6.00
6	≥ 20	≤ 46	143	0.57	139	35.12	6.51

c)

Drainage class	Depth of mottling (cm)	Drainage level	Count	Geometric Mean $\chi_{LF} \times 10^{-6}$ m^3 kg^{-1}	Count	Geometric Mean $\chi_{FD} \times 10^{-9}$ m^3 kg^{-1}	Mean χ_{FD}%
1	≥ 0 - 25	Poorly drained (including peats)	1410	0.24	1159	7.71	3.04
2	> 25 - 40	Poor-intermediate	664	0.31	615	10.75	3.59
3	> 40 - 80	Intermediate-free	516	0.39	497	14.85	4.19
4	> 80 or no mottling	Free draining	2306	0.59	2264	32.11	5.76

Table 5

a)

Category	Count	Geometric Mean $\chi_{LF} \times 10^{-6}\ m^3\ kg^{-1}$	Category	Count	Geometric Mean $\chi_{FD} \times 10^{-9}\ m^3\ kg^{-1}$	Category	Count	Mean χ_{FD}%
humose clays	28	0.60	humose clays	28	24.74	humose medium silts	75	5.69
medium loams	1623	0.53	humose medium silts	75	22.99	humose light silts	22	5.33
medium silts	868	0.48	medium loams	1610	22.05	medium silts	863	5.13
light silts	138	0.45	medium silts	863	21.28	light silts	138	5.06
humose medium silts	85	0.41	light silts	138	19.87	medium loams	1610	4.81
clays	383	0.37	humose light silts	22	18.60	humose clays	28	4.75
humose light loams	147	0.37	humose medium loams	89	16.32	humose medium loams	89	4.59
humose medium loams	100	0.37	humose light loams	131	14.89	light loams	807	4.33
light loams	831	0.36	light loams	807	14.59	humose light loams	131	4.13
humose light silts	25	0.31	clays	381	11.97	sands	142	4.07
sands	150	0.27	sands	142	11.23	clays	381	3.78
peats	480	0.17	peats	228	10.54	humose sands	21	3.63
humose sands	38	0.11	humose sands	21	6.23	peats	228	3.38

b)

Land use	Count	Geometric Mean $\chi_{LF} \times 10^{-6}\ m^3\ kg^{-1}$	Land use	Count	Geometric Mean $\chi_{FD} \times 10^{-9}\ m^3\ kg^{-1}$	Land use	Count	Mean χ_{FD}%
ley grassland	615	0.56	ley grassland	610	25.24	ley grassland	610	5.19
horticultural crops	30	0.52	scrub	68	24.63	scrub	68	5.14
other	30	0.50	other	27	24.06	deciduous	220	4.82
scrub	71	0.49	horticultural crops	30	21.42	coniferous	144	4.74
recreation	34	0.45	arable	1631	18.51	arable	1631	4.65
arable	1633	0.45	deciduous	220	17.23	other	27	4.65
permanent grassland	1347	0.45	permanent grassland	1327	17.15	horticultural crops	30	4.55
deciduous	230	0.39	recreation	33	15.84	rough grazing	174	4.43
orchard	30	0.33	coniferous	144	14.46	permanent grassland	1327	4.43
not recorded	54	0.32	rough grazing	174	13.76	not recorded	50	4.38
rough grazing	241	0.24	not recorded	50	12.44	lowland heath	9	3.97
coniferous	192	0.24	orchard	30	11.76	upland grass	103	3.86
salt marsh	5	0.18	upland grass	103	10.07	orchard	30	3.84
upland heath	104	0.17	lowland heath	9	8.09	recreation	33	3.61
upland grass	209	0.17	upland heath	61	6.55	upland heath	61	2.90
lowland heath	17	0.15	salt marsh	4	4.89	salt marsh	4	2.19
bog	54	0.11	bog	14	4.19	bog	14	2.03

Table 6

a)

% OC Class	Lower boundary	Upper boundary	Geometric Mean $\chi_{LF} \times 10^{-6}$ m^3 kg^{-1}	Geometric Mean $\chi_{FD} \times 10^{-9}$ m^3 kg^{-1}	Mean χ_{FD}%
1	≥ 0.1	< 1.5	0.34	12.63	4.14
2	≥ 1.5	< 2	0.35	13.03	4.14
3	≥ 2	< 2.5	0.40	15.62	4.45
4	≥ 2.5	< 3	0.42	16.60	4.44
5	≥ 3	< 3.5	0.48	20.59	4.92
6	≥ 3.5	< 4.2	0.54	25.50	5.24
7	≥ 4.2	< 5.1	0.54	24.53	5.00
8	≥ 5.1	< 6.7	0.48	20.64	4.83
9	≥ 6.7	< 12.1	0.41	17.44	4.55
10	≥ 12.1	< 31	0.29	16.06	4.28
11	≥ 31	< 47.6	0.13	6.84	2.38
12	≥ 47.6	≤ 65.5	0.11	9.14	2.74

b)

pH Class	Lower boundary	Upper boundary	Geometric Mean $\chi_{LF} \times 10^{-6}$ m^3 kg^{-1}	Geometric Mean $\chi_{FD} \times 10^{-9}$ m^3 kg^{-1}	Mean χ_{FD}%
1	≥ 3.0	< 3.5	0.12	4.93	2.14
2	≥ 3.5	< 4.0	0.18	9.96	3.78
3	≥ 4.0	< 4.5	0.29	17.56	4.82
4	≥ 4.5	< 5.0	0.39	18.16	4.79
5	≥ 5.0	< 5.5	0.48	20.01	4.77
6	≥ 5.5	< 6.0	0.50	20.17	4.68
7	≥ 6.0	< 6.5	0.44	16.20	4.21
8	≥ 6.5	< 7.0	0.39	14.20	3.98
9	≥ 7.0	< 7.5	0.45	18.12	4.51
10	≥ 7.5	< 8.0	0.47	21.43	5.19
11	≥ 8.0	< 8.5	0.36	14.79	4.48
12	≥ 8.5	≤ 9.2	0.17	2.83	1.49

Table 7

Area Number	Count	Geometric Mean $\chi_{LF} \times 10^{-6}$ m^3 kg^{-1}	Count	Geometric Mean $\chi_{FD} \times 10^{-9}$ m^3 kg^{-1}	Mean χ_{FD}%
1	1561	0.49	1514	23.58	5.28
2	1762	0.40	1539	14.31	4.03
3	1573	0.34	1482	16.72	4.50

Table 8

Factor	$\log_{10} \chi_{LF} \times 10^{-6}$ m^3 kg^{-1}	Factor	$\log_{10} \chi_{FD} \times 10^{-9}$ m^3 kg^{-1}	Factor	χ_{FD}%
Parent material	0.48 (0.23)	*Parent material*	0.51 (0.26)	*Parent material*	0.50 (0.25)
Drainage	0.38 (0.14)	*Drainage*	0.4 (0.16)	*Drainage*	0.43 (0.19)
Texture	0.34 (0.11)	*logMAR*	0.24 (0.06)	*logSlope*	0.26 (0.07)
Land use	0.33 (0.11)	*logSlope*	0.23 (0.05)	*logMAR*	0.24 (0.06)
logrMAT	0.21 (0.04)	*Texture*	0.17 (0.03)	*Time*	0.19 (0.03)
pH	0.17 (0.03)	*Land use*	0.15 (0.02)	*Texture*	0.18 (0.03)
logOC	-0.17 (0.03)	*Time*	0.14 (0.02)	*logAlt*	0.16 (0.03)
logSlope	0.14 (0.02)	*logAlt*	0.14 (0.02)	*Land use*	0.14 (0.02)
Time	0.14 (0.02)	*logrMAT*	0.06 (0.00)	*logrMAT*	0.05 (0.00)
logMAR	0.05 (0.00)	*pH*	0.04 (0.00)	*pH*	0.04(0.00)*
logAlt	N/S	*logOC*	0.04 (0.00)	*logOC*	N/S

Table 9

a) Model 1 $\log_{10} \chi_{LF} \times 10^{-6}$ m^3 kg^{-1}

n = 4896, R^2 = 0.389, Adjusted R^2 = 0.388, RMSE = 0.360

						r			r^2		
	B	Std. Error	Beta	t	Sig.	Zero-order	Partial	Part	Zero-order	Partial	Part
(Constant)	-0.589	0.166		-3.538	0.000						
Parent material	0.710	0.027	0.341	26.674	0.000	0.480	0.357	0.298	0.231	0.127	0.089
Drainage	0.618	0.034	0.232	18.031	0.000	0.376	0.250	0.202	0.141	0.062	0.041
Land use	0.695	0.050	0.226	13.857	0.000	0.325	0.194	0.155	0.106	0.038	0.024
Texture	0.476	0.044	0.161	10.809	0.000	0.338	0.153	0.121	0.114	0.023	0.015
logOC	0.202	0.024	0.141	8.586	0.000	-0.170	0.122	0.096	0.029	0.015	0.009
logMAR	0.404	0.054	0.130	7.471	0.000	0.052	0.106	0.084	0.003	0.011	0.007
logAlt	-0.089	0.016	-0.101	-5.681	0.000	-0.010	-0.081	-0.064	0.000	0.007	0.004
pH	0.020	0.005	0.057	3.636	0.000	0.172	0.052	0.041	0.030	0.003	0.002
logSlope	0.054	0.017	0.046	3.157	0.002	0.141	0.045	0.035	0.020	0.002	0.001
logrMAT	0.215	0.081	0.051	2.660	0.008	0.206	0.038	0.030	0.043	0.001	0.001
Time	-0.002	0.105	0.000	-0.019	0.985	0.143	0.000	0.000	0.020	0.000	0.000

b) Model 1 χ_{FD}%

n = 4535, R^2 = 0.362, Adjusted R^2 = 0.360, RMSE = 2.22

						r			r^2		
	B	Std. Error	Beta	*t*	Sig.	Zero-order	Partial	Part	Zero-order	Partial	Part
(Constant)	-17.381	1.183		-14.690	0.000						
Parent material	0.684	0.029	0.341	23.954	0.000	0.499	0.336	0.284	0.249	0.113	0.081
Drainage	0.637	0.033	0.264	19.331	0.000	0.432	0.276	0.230	0.187	0.076	0.053
logMAR	2.862	0.366	0.139	7.827	0.000	0.245	0.116	0.093	0.060	0.013	0.009
Land use	0.712	0.092	0.100	7.757	0.000	0.141	0.115	0.092	0.020	0.013	0.008
pH	0.224	0.034	0.100	6.564	0.000	0.037	0.097	0.078	0.001	0.009	0.006
logAlt	-0.565	0.098	-0.102	-5.778	0.000	0.163	-0.086	-0.069	0.027	0.007	0.005
Texture	0.392	0.068	0.072	5.732	0.000	0.184	0.085	0.068	0.034	0.007	0.005
Time	0.362	0.077	0.067	4.710	0.000	0.186	0.070	0.056	0.034	0.005	0.003
logSlope	0.466	0.110	0.065	4.239	0.000	0.259	0.063	0.050	0.067	0.004	0.003
logOC	0.319	0.161	0.028	1.974	0.048	0.008	0.029	0.023	0.000	0.001	0.001
logrMAT	-0.163	0.473	-0.006	-0.344	0.731	0.045	-0.005	-0.004	0.002	0.000	0.000

Table 10

a) Model 2a $\log_{10} \chi_{LF} \times 10^{-6}$ m^3 kg^{-1}

n = 4129, R^2 = 0.400, Adjusted R^2 = 0.397, RMSE = 0.333

						r			r^2		
	B	Std. Error	Beta	t	Sig.	Zero-order	Partial	Part	Zero-order	Partial	Part
(Constant)	-0.615	0.191		-3.229	0.001						
Parent material	0.775	0.026	0.409	29.615	0.000	0.528	0.410	0.349	0.279	0.168	0.122
Drainage	0.685	0.037	0.246	18.534	0.000	0.359	0.271	0.218	0.129	0.073	0.048
Texture	0.633	0.061	0.129	10.372	0.000	0.203	0.156	0.122	0.041	0.024	0.015
Land use	0.770	0.077	0.128	10.055	0.000	0.166	0.151	0.118	0.028	0.023	0.014
logMAR	0.403	0.058	0.122	6.958	0.000	0.266	0.105	0.082	0.071	0.011	0.007
logOC	0.198	0.030	0.089	6.542	0.000	0.108	0.099	0.077	0.012	0.010	0.006
pH	0.034	0.005	0.096	6.352	0.000	0.024	0.096	0.075	0.001	0.009	0.006
logrMAT	0.335	0.077	0.075	4.348	0.000	0.098	0.066	0.051	0.010	0.004	0.003
logAlt	-0.043	0.015	-0.048	-2.780	0.005	0.143	-0.042	-0.033	0.021	0.002	0.001
logSlope	0.018	0.017	0.016	1.056	0.291	0.211	0.016	0.012	0.044	0.000	0.000
Time	-0.052	0.111	-0.007	-0.469	0.639	0.130	-0.007	-0.006	0.017	0.000	0.000

b) Model 2a χ_{FD}%

n = 4061, R^2 = 0.371, Adjusted R^2 = 0.369, RMSE = 2.20

						r			r^2		
	B	Std. Error	Beta	t	Sig.	Zero-order	Partial	Part	Zero-order	Partial	Part
(Constant)	-17.066	1.271		-13.428	0.000						
Parent material	0.679	0.028	0.353	23.897	0.000	0.519	0.344	0.291	0.269	0.118	0.085
Drainage	0.615	0.032	0.266	19.275	0.000	0.433	0.283	0.234	0.187	0.080	0.055
logMAR	3.085	0.391	0.143	7.883	0.000	0.312	0.120	0.096	0.097	0.014	0.009
pH	0.257	0.035	0.110	7.349	0.000	-0.009	0.112	0.089	0.000	0.013	0.008
Time	0.384	0.076	0.072	5.021	0.000	0.188	0.077	0.061	0.035	0.006	0.004
Texture	0.360	0.079	0.057	4.536	0.000	0.159	0.069	0.055	0.025	0.005	0.003
Land use	0.467	0.123	0.047	3.802	0.000	0.010	0.058	0.046	0.000	0.003	0.002
logAlt	-0.376	0.101	-0.065	-3.732	0.000	0.215	-0.057	-0.045	0.046	0.003	0.002
logSlope	0.361	0.113	0.050	3.195	0.001	0.279	0.049	0.039	0.078	0.002	0.002
logOC	0.241	0.201	0.017	1.200	0.230	0.083	0.018	0.015	0.007	0.000	0.000
logrMAT	0.184	0.470	0.006	0.390	0.696	0.008	0.006	0.005	0.000	0.000	0.000

c) Model 2b $\log_{10} \chi_{LF} \times 10^{-6}$ m^3 kg^{-1}

n = 4129, R^2 = 0.452, Adjusted R^2 = 0.450, RMSE = 0.319

	B	Std. Error	Beta	t	Sig.	r Zero-order	r Partial	r Part	r^2 Zero-order	r^2 Partial	r^2 Part
(Constant)	-0.279	0.188		-1.486	0.137						
Parent material	0.694	0.026	0.370	26.896	0.000	0.533	0.387	0.310	0.284	0.149	0.096
logCSand	0.343	0.018	0.263	18.888	0.000	0.459	0.282	0.218	0.211	0.080	0.048
Drainage	0.501	0.038	0.179	13.306	0.000	0.357	0.203	0.154	0.127	0.041	0.024
Texture	0.679	0.059	0.140	11.564	0.000	0.207	0.177	0.133	0.043	0.031	0.018
Landuse	0.750	0.075	0.124	9.981	0.000	0.166	0.154	0.115	0.027	0.024	0.013
logOC	0.207	0.031	0.091	6.785	0.000	0.114	0.105	0.078	0.013	0.011	0.006
pH	0.029	0.005	0.080	5.406	0.000	0.022	0.084	0.062	0.001	0.007	0.004
logAlt	-0.081	0.015	-0.090	-5.285	0.000	0.148	-0.082	-0.061	0.022	0.007	0.004
logMAR	0.204	0.058	0.061	3.504	0.000	0.271	0.055	0.040	0.074	0.003	0.002
logrMAT	0.231	0.076	0.052	3.030	0.002	0.102	0.047	0.035	0.010	0.002	0.001
logSlope	-0.006	0.017	-0.005	-0.357	0.721	0.214	-0.006	-0.004	0.046	0.000	0.000
Time	0.033	0.101	0.005	0.327	0.744	0.141	0.005	0.004	0.020	0.000	0.000

d) Model 2b χ_{FD}%

n = 4061, R^2 = 0.395, Adjusted R^2 = 0.393, RMSE = 2.167

	B	Std. Error	Beta	t	Sig.	r Zero-order	r Partial	r Part	r^2 Zero-order	r^2 Partial	r^2 Part
(Constant)	-14.970	1.284		-11.658	0.000						
Parent material	0.610	0.029	0.316	20.905	0.000	0.518	0.312	0.256	0.268	0.097	0.065
Drainage	0.505	0.033	0.216	15.084	0.000	0.427	0.231	0.184	0.182	0.053	0.034
logCSand	1.635	0.124	0.195	13.210	0.000	0.435	0.203	0.161	0.189	0.041	0.026
pH	0.245	0.035	0.104	6.911	0.000	-0.006	0.108	0.084	0.000	0.012	0.007
Texture	0.460	0.076	0.076	6.030	0.000	0.166	0.094	0.074	0.028	0.009	0.005
Time	0.403	0.073	0.080	5.542	0.000	0.199	0.087	0.068	0.040	0.008	0.005
logMAR	2.170	0.402	0.100	5.399	0.000	0.314	0.085	0.066	0.098	0.007	0.004
logAlt	-0.544	0.102	-0.094	-5.323	0.000	0.216	-0.083	-0.065	0.047	0.007	0.004
Landuse	0.436	0.120	0.045	3.634	0.000	0.103	0.057	0.044	0.011	0.003	0.002
logSlope	0.273	0.114	0.038	2.392	0.017	0.281	0.038	0.029	0.079	0.001	0.001
logrMAT	-0.380	0.475	-0.013	-0.800	0.424	0.010	-0.013	-0.010	0.000	0.000	0.000
logOC	0.163	0.208	0.011	0.782	0.434	0.081	0.012	0.010	0.007	0.000	0.000

Table 11

a) Model 3 $\log_{10} \chi_{LF} \times 10^{-6}$ m^3 kg^{-1}

n = 2047, R^2 = 0.461, Adjusted R^2 = 0.458, RMSE = 0.331

						r			r^2		
	B	Std. Error	Beta	t	Sig.	Zero-order	Partial	Part	Zero-order	Partial	Part
(Constant)	-1.076	0.263		-4.098	0.000						
Parent material	0.736	0.034	0.422	21.685	0.000	0.573	0.433	0.353	0.328	0.187	0.125
logCSand	0.389	0.025	0.280	15.429	0.000	0.464	0.324	0.251	0.215	0.105	0.063
Texture	0.408	0.058	0.122	7.014	0.000	0.300	0.154	0.114	0.090	0.024	0.013
pH	0.032	0.007	0.086	4.297	0.000	-0.080	0.095	0.070	0.006	0.009	0.005
logrMAT	0.420	0.099	0.091	4.240	0.000	0.102	0.094	0.069	0.010	0.009	0.005
logSlope	-0.090	0.023	-0.079	-3.961	0.000	0.179	-0.087	-0.064	0.032	0.008	0.004
Landuse	0.341	0.093	0.061	3.644	0.000	0.181	0.081	0.059	0.033	0.007	0.003
logMAR	0.286	0.084	0.085	3.380	0.001	0.354	0.075	0.055	0.125	0.006	0.003
logOC	0.141	0.046	0.060	3.067	0.002	0.252	0.068	0.050	0.064	0.005	0.003
Time	0.111	0.089	0.023	1.240	0.215	0.212	0.027	0.020	0.045	0.001	0.000
logAlt	0.016	0.026	0.013	0.596	0.551	0.173	0.013	0.010	0.030	0.000	0.000

b) Model 3 χ_{FD}%

n = 2037, R^2 = 0.376, Adjusted R^2 = 0.373, RMSE = 2.162

						r			r^2		
	B	Std. Error	Beta	t	Sig.	Zero-order	Partial	Part	Zero-order	Partial	Part
(Constant)	-12.634	1.639		-7.710	0.000						
Parent material	0.711	0.040	0.368	17.876	0.000	0.517	0.369	0.314	0.267	0.136	0.099
logCSand	1.872	0.164	0.223	11.442	0.000	0.392	0.246	0.201	0.154	0.061	0.040
Time	0.434	0.067	0.131	6.439	0.000	0.303	0.142	0.113	0.092	0.020	0.013
Texture	0.378	0.068	0.109	5.529	0.000	0.288	0.122	0.097	0.083	0.015	0.009
pH	0.220	0.049	0.099	4.510	0.000	-0.025	0.100	0.079	0.001	0.010	0.006
logMAR	2.135	0.544	0.106	3.924	0.000	0.328	0.087	0.069	0.108	0.008	0.005
Landuse	0.194	0.139	0.025	1.393	0.164	0.131	0.031	0.024	0.017	0.001	0.001
logAlt	-0.265	0.173	-0.037	-1.533	0.125	0.179	-0.034	-0.027	0.032	0.001	0.001
logSlope	-0.141	0.150	-0.020	-0.939	0.348	0.203	-0.021	-0.016	0.041	0.000	0.000
logrMAT	0.342	0.635	0.012	0.538	0.590	0.061	0.012	0.009	0.004	0.000	0.000
logOC	0.153	0.306	0.011	0.500	0.617	0.237	0.011	0.009	0.056	0.000	0.000

Table 12

Fe class	Fe mg kg^{-1} Lower boundary	Upper boundary	Geometric Mean $\chi_{LF} \times 10^{-6}$ m^3 kg^{-1}	Geometric Mean $\chi_{FD} \times 10^{-9}$ m^3 kg^{-1}	Mean χ_{FD}%
1	395	10180	0.13	5.68	3.25
2	10180	15839	0.25	9.67	4.00
3	15839	20195	0.30	10.71	3.90
4	20195	23699	0.31	10.53	3.79
5	23699	26717.5	0.36	13.80	4.20
6	26717.5	30030	0.42	15.77	4.26
7	30030	33584.5	0.43	16.55	4.40
8	33584.5	38088	0.56	23.66	4.93
9	38088	44374	0.79	40.44	5.73
10	44374	50301.25	1.12	72.47	6.99
11	50301.25	264405	1.25	79.02	7.01
12	264405	58538	1.00	55.70	5.80

Table 13

a)

Major Soil Group	Count	Geometric mean $\chi_{LF} \times 10^{-6}$ m^3 kg^{-1}	Major Soil Group	Count	Geometric mean $\log_{10} \chi_{FD} \times 10^{-9}$ m^3 kg^{-1}	Major Soil Group	Count	Mean $\chi_{FD\%}$
Lithomorphic	373	0.67	Podzolic	383	49.46	Lithomorphic	357	6.89
Podzolic	451	0.60	Lithomorphic	357	46.33	Podzolic	383	6.53
Man-made	94	0.53	Brown soils	1839	23.49	Brown soils	1839	5.14
Brown soils	1846	0.51	Man-made	93	21.14	Man-made	93	4.31
Pelosols	224	0.35	Peat	56	14.66	Pelosols	223	3.65
Groundwater gleys	519	0.28	Pelosols	223	11.11	Peat	56	3.34
Surface water gleys	1204	0.27	Surface water gleys	1081	8.56	Surface water gleys	1081	3.24
Terrestrial raw	16	0.19	Groundwater gleys	485	8.29	Groundwater gleys	485	3.12
Peat	164	0.17	Terrestrial raw	15	3.57	Terrestrial raw	15	1.87
Raw gley	5	0.12	Raw gley	3	3.17	Raw gley	3	1.58

b)

Subgroup top 10			Subgroup top 10			Subgroup top 10		
Typical brown podzolic	224	1.77	Typical brown podzolic	223	142.44	Typical brown podzolic	223	8.34
Brown ranker	72	1.22	Brown ranker	71	81.81	Brown rendzina	164	7.68
Brown rendzina	164	0.83	Brown rendzina	164	61.22	Brown ranker	71	6.96
Typical brown earths	504	0.81	Typical brown earths	502	47.38	Grey rendzina	40	6.59
Stagnogleyic brown earths	133	0.72	Stagnogleyic brown earths	133	38.58	Typical brown earths	502	6.27
Typical brown calcareous earths	193	0.60	Typical brown calcareous earths	193	35.18	Typical brown calcareous earths	193	6.23
Typical humic-alluvial gley	31	0.58	Typical humic-alluvial gley	28	30.81	Stagnogleyic brown earth	133	5.95
Disturbed soils	67	0.50	Gleyic brown earths	74	22.54	Gleyic brown earths	74	5.08
Gleyic brown earths	76	0.48	Grey rendinas	40	22.54	Typical paleo-agrillic brown earths	94	4.95
Typical paleo-agrillic brown earths	91	0.42	Typical paleo-agrillic brown earths	94	19.55	Argillic brown sands	32	4.81

Subgroup lowest 10			Subgroup lowest 10			Subgroup lowest 10		
Gleyic argillic brown earths	39	0.24	Calcareous alluvial gley	58	7.00	Typical argillic pelosols	37	2.99
Typical argillic gley soils	38	0.21	Typical alluvial gley	78	6.67	Typical argillic gley soils	36	2.97
Ironpan stagnopodzols	46	0.16	Typical stagnogley	478	6.59	Humo-ferric podzols	25	2.84
Typical sandy gley soils	26	0.16	Pelo alluvial gley	88	6.37	Typical alluvial gley	78	2.84
Humo-ferric podzols	35	0.15	Gleyic argillic brown earths	39	6.21	Calcareous alluvial gley	58	2.82
Raw oligo-amorphous peat	30	0.14	Humo-ferric podzols	25	6.01	Typical stagnogley	478	2.81
Cambic stagnohumic gley	155	0.13	Typical argillic gley soils	36	5.43	Pelo alluvial gley	88	2.59
Typical humic gley	29	0.13	Pelo-calcareous alluvial gley	27	4.71	Cambic stagnohumic gley	67	2.24
Raw oligo-fibrous peat	93	0.12	Cambic stagnohumic gley	67	4.51	Typical sandy gley soils	25	2.22
Stagnogley podzol	24	0.10	Typical sandy gley soils	25	3.51	Pelo-calcareous alluvial gley	27	2.04